Small-scale Landform Classification and Flood Susceptibility Assessment of the Alluvial Plains in Vietnam Using Remotely Sensed Data

(リモートセンシングデータを用いたベトナムの沖積平野の微地形分類および洪水危険度評価)

HO, Loan Thi Kim

A dissertation for the degree of Doctor of Environmental Studies

Department of Earth and Environmental Sciences,

Graduate School of Environmental Studies, Nagoya University

(名古屋大学大学院環境学研究科地球環境科学専攻学位論文　博士　(環境学))

2013

Table of Contents

List of Figures

List of Tables

SUMMARY

Global warming has increased precipitation intensity and variability that lead to induce the risks of flooding and drought in many areas. In Vietnam, frequency and intensiveness of the natural disasters such as typhoon, heavy rain, floods, high temperature, and drought are increasing in many regions of the country. Annual average temperature increases about 0.1 ^{o}C per decade observed from 1974 to 2004 (National Institute of Meteorology, Hydrology and Environment, 2007). Heavy rain occurs more frequently and seasonal rainfall amount decreases in July and August (dry season) whereas increases in September, October, and November (rainy season).

Floods are the most catastrophic natural disaster that occurs in Vietnam; they result from the typical tropical monsoon climatic features exacerbated by topographic characteristics and recent climate change (CCFSC, 2006). Flood hazard mapping is therefore a crucial tool for monitoring the flood risk in this region. Flood inundation is caused naturally by meteorological and hydrological factors, and its occurrence in alluvial floodplains can be understood by studying the geomorphological characteristics of those plains. Alluvial plains are often ideal locations for human settlement and urbanization, particularly on natural levees and alluvial terraces, which are typically above the level of flooding; however, poorly implemented settlement can result in flood vulnerability. Studies on landform characteristics in floodplains can help explain and monitor flood inundation states and provide valuable information for land use and urban planning (Oya, 2001). Although the land surface in floodplain settlements has often been substantially altered by the built environment, flood inundation tends to occur relative to the structure of the original landforms.

For those reasons mentioned above, the **overarching objective** of this study is to assess flood susceptibility based on the geomorphological approach by using remotely sensed data. The first important step in flood susceptibility zonation using this approach is detailed geomorphological mapping, also called landform classification.

Sub-objective 1: Generation of a manual landform classification map by visual interpretation for zoning flood susceptibility (a case study in central Vietnam).

The first part of this study (Chapter 2) developed an integrated method for classifying small-scale landforms and flood hazard zones based on a geomorphological approach utilizing Shuttle Radar Topographic Mission Digital Elevation Model (SRTM DEM) and Landsat ETM+ (Enhanced Thematic Mapper Plus) data combined with field investigation. Small-scale landform units on an alluvial plain were classified in relation to flood conditions by integrating an SRTM DEM with spectral characteristics from a pair of Landsat images from dry and flood seasons. In addition, the Landsat ETM+ band 4-band 3 of the flood season image was calculated to identify moist surfaces.

Next, a flood susceptibility zonation map was generated by categorizing geomorphological features and the average elevation of each landform into flood hazard classes. Then, three-dimensional (3D) diagrams of the composed maps were produced using Geographical Resources Analysis Support System (GRASS) 6.3 to visualize the geomorphology and flooding risk. The results were validated using field surveys, topographic maps, and past inundation images. This case study was undertaken for the Thu Bon alluvial plain, central Vietnam. The findings of this study revealed a close interaction between the geomorphological characteristics of this region and flood conditions. Flooding and sedimentation mechanisms cause dynamic formations of fluvial and coastal landforms, and these geomorphological features in

turn affect flood hazard. Furthermore, 43.34% of the area of this plain is classified as having a very high or high flood hazard in lowland areas and a flashflood susceptibility in higher areas.

Sub-objective 2: Development of a rule-based digital method for small-scale landform classification related to flood conditions for facilitating the manual landform classification procedure that is often known as time-consuming, subjective, and difficult to edit (the case study in central Vietnam).

The second part of this study (Chapter 3) developed a rule-based digital method for generating a landform classification map of an alluvial plain for further assessment of flood susceptibility. The rule-based digital method for classifying landforms is based on characteristics of land cover and thresholds of land-surface parameters. These inputs are combined by using a rule. Thresholds of the Modified Normalized Difference Water Index (MNDWI) and land cover characteristics were extracted from Landsat and Advanced Spaceborne Thermal Emission and Reflection Radiometer (ASTER) data. Local relief, average elevation, and channel features were calculated using SRTM DEM. Then, relative position indices of polygons were used to classify small-scale landform objects. The landform classification map by this method was compared to a manual classification map by visual interpretation that is often time-consuming, subjective, and inconvenient to edit. Significant consistence of dominated landform categories between the two maps demonstrates the effectiveness of the rule-based digital method despite the limitation on spatial resolution of medium-resolution data for detecting some small features. Moreover, the remarkable merits of the rule-based digital method in comparison with the manual method are its relative time savings, objectivity, and ease of editing.

<u>Sub-objective 3:</u> Generalization of the rule-based digital landform classification method for wider applications (a case study in Hanoi area, north Vietnam).

The third part of this study (Chapter 4) describes the adaptation of the rule-based digital landform classification method, reported above, to local topographic characteristics in the western plain of the Red River delta, northern Vietnam. This part attempts to generalize this rule-based method for wider applications in other alluvial plains. The original classification scheme was generally based on the moist condition classification, local land-surface parameters, and relative position indices derived from multi-temporal Landsat data and a SRTM DEM. This study used average elevations and the standard deviation of elevations as local land-surface parameters rather than local relief, which was used in the second part. Multi-temporal land cover classification was performed using an integrated method to effectively enhance the SRTM DEM. The overall classification was consistent with manual mapping by visual comparison. The quantitative comparison between landform units and past flood-affected areas demonstrated a precise boundary delineation of landform objects using this method.

CHAPTER 1 – General introduction

1.1 Background of flood disasters

Flood is known as the most catastrophic disaster all over the world among hydrometeorological disasters and the number of flood events have been increasing for several last decades (International Strategy for Disaster Reduction - ISDR) (Fig. 1). During 1980-2008, approximately 2.8 billion people are affected by floods worldwide (96 million people per year) (EM-DAT, 2008, at http://www.emdat.be/).

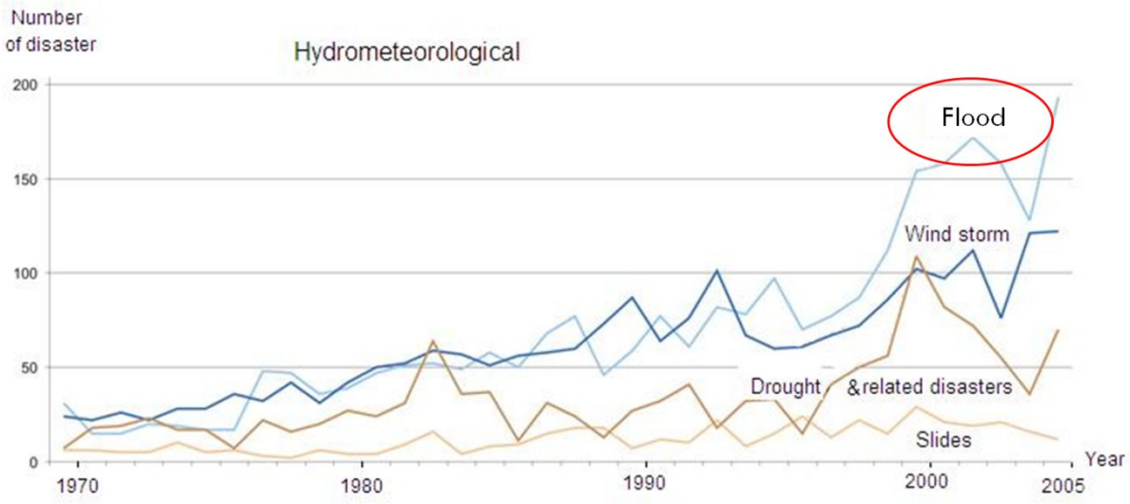

Fig. 1. Number of natural disasters by type in the world 1970-2005 (ISDR).

Asia has the highest flood hazard number potential with 1179 flood occurrence events (among 2887 events of natural disasters worldwide) during 1980-2008 (EM-DAT, 2008, at http://www.emdat.be/) (Fig. 2). For the past two decades, approximately more than 400 million people have been affected by floods. During 1987 - 1997, flood in Asia accounted for 44% of all flood disasters in the world and caused 228,000 losses of human lives (approximately 93% of all flood-related deaths worldwide). Totaled US

$136 billion was lost in Asia in that decade. Particularly, in South-East Asia, flood is a well-known phenomenon.

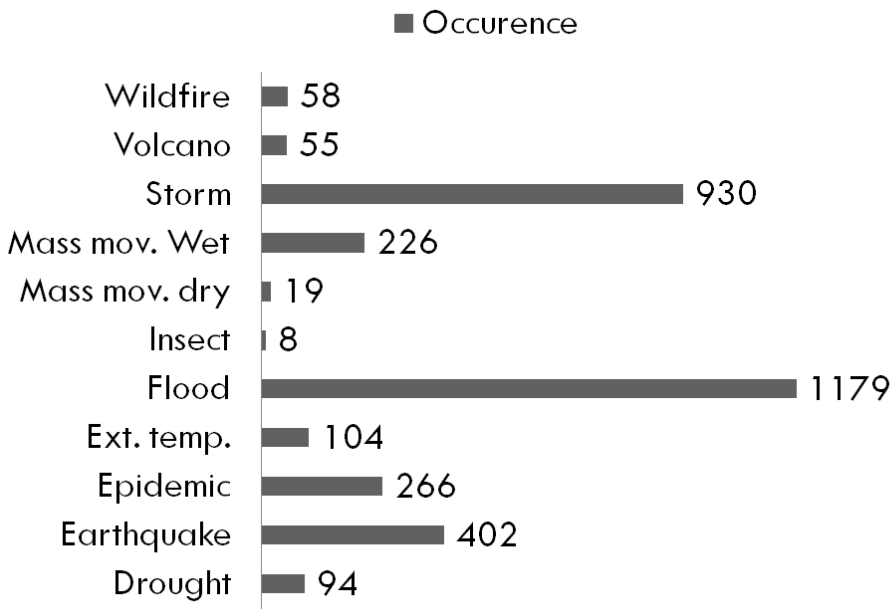

Fig. 2. Natural disaster occurrence reported in Asia during 1980-2008. Source: EM-DAT, 2008, at http://www.emdat.be/.

In Vietnam, flood is one of the two most catastrophic disasters, along with storm (Fig. 3). Flood causes numerous human lives and economic losses to the country every year. Vietnam ranks third (among 162 countries) in percentage of people exposed to flood per year (3.9 % - 3.4 million people) and GDP exposure per year (4 % - 2.2 billion USD) (Global Assessment Report, 2009).

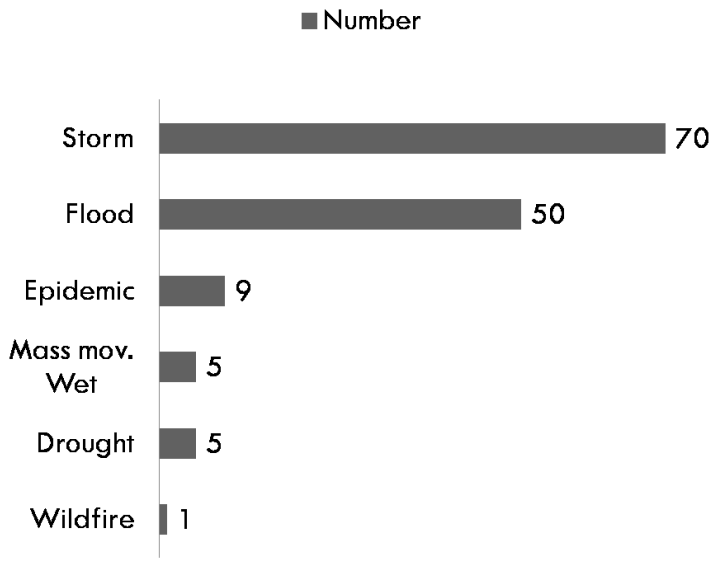

Fig. 3. Natural disaster occurrence reported in Vietnam during 1980 – 2008. Source: Global Assessment Report, 2009.

Flood in Vietnam results from the typical tropical monsoon climatic features exacerbated by topographic characteristics and recent climate change (CCFSC, 2006). Major floods occur more frequently than ever (1964, 1999, 2007, 2008, 2009, and 2010).

Located in eastern Indochina, Vietnam has elongated shape with the coastline stretching across 3260 km in length and the Truong Son Mountain Range in the West. Along with two major large plains, Red River delta in north and Mekong River delta south Vietnam, the central coastal plains are characterized by narrow shape with short and steep rivers. The low coastal zone of Vietnam has suffered flood disaster almost every year (Fig. 4).

Fig. 4. Natural disaster map of Vietnam (CCFSC, 2006)

Annual rainfall ranges from 1800 to 2500 mm (approximately 3000 mm in central Vietnam), but is distributed unevenly in a year (more than 70% of annual rainfall occurs in a rainy season from July to September) that is one of the main causes of riverine flooding (CCFSC, 2006).

1.2 Situations of flood response and researches on flood hazard mapping in Vietnam

Because of settling down and developing at low-lying river deltas and coastal lands and wet-rice agriculture as main livelihood activities, most of the population of Vietnam has frequently been confronted with serious flood disasters. Rapid population

growth in recent years, the reckless settlements and installation of economic activities in flood hazardous areas without risk consideration and lack of adequate financial support to improve disaster management programs lead a lot of people to be vulnerable to flood hazard (Imamura and Dang, 1997). On the other hand, the fact that available flood hazard maps in Vietnam show flood inundated areas quite roughly, and most researches focus on Mekong River delta (south), Red River delta (north), and Hue (central) (e.g., Shida and Haruyama, 2004; Hori et al., 2004; Haruyama and Shida, 2008; Tran et al., 2008; Nguyen et al., 2011; Funabiki et al., 2012), generating more detailed flood hazard maps is necessary. Predicting flood-prone areas based on a geomorphological point of view is rather undeveloped in Vietnam, but it is supposed to be able to create more detailed flood-prone areas.

A flood hazard map is a very important non-structure measure for evacuation, flood damage mitigation, and land use planning. Although the dike systems were constructed in some big river such as the Red River in north Vietnam, the risk of dike breaking is recognized in case of a big flood. The flood hazard map can provide scenarios of flood inundation when dike breaking. The maps can provide valuable information to save human lives and properties of people in floodplains and contribute to suitable urban development planning. In fact, however, flood mapping researches in Vietnam has been restricted due to several problems that are discussed in sections 1.3 and 1.4 below.

1.3 Why flood hazard mapping based on geomorphological approaches?

There are several methods for flood mapping that are based primarily on hydrological, meteorological, and geomorphological approaches (e.g., Kenny, 1990; Ballais et al., 2005). In developing countries, where hydro-meteorological data or/and high-resolution satellite images are commonly insufficient, thus limiting the generation

of flood models, the geomorphological method is most effective and appropriate (Wolman, 1971; Lastra et al., 2008). Moreover, obtaining past flood images for generating flood hazard maps is normally a difficult task, particularly in developing countries, where high-resolution, active remote sensing imagery, such as Radar, are difficult to obtain. Passive optical imagery is often unusable during floods because of cloud coverage. In addition, capturing the exact time of flood occurrence is difficult due to repetition cycles of satellites. The geomorphological method uses aerial photo interpretation and field investigations of flood evidences to study geomorphological characteristics in relation to historical flood events (Baker et al., 1988). A geomorphological map can assist with studying the extent of inundated areas, the direction of flood flow, and changes in river channels through examination of remnant flood evidences, relief features, and deposits formed by repeated flooding. Such maps can also reveal the nature of former floods and the probable characteristics of floods occurring in the future (Lastra et al., 2008; Oya, 2002). A landform classification map plays an important role in the study of the characteristics of many natural phenomena because of the relationship between landforms and these phenomena on a landform element level, for example, in the case of floods, landslides, and erosion (Speight, 1990). Studies on landform characteristics in floodplains can help explain and monitor flood inundation states and provide valuable information for land use and urban planning (Oya, 2001; Speight, 1990). This approach to flood investigation has been verified in the case where a channel system and the associated floodplain morphology experience dynamic changes resulting in highly erosive potential and substantial sediment supply (Lastra et al., 2008). It is therefore suitable to study flooding in the alluvial plains of Vietnam where fluvial morphology alters frequently.

Steps in flood hazard assessment by the geomorphological approach: (1) mapping detailed geomorphological features, (2) defining flood susceptibility of each geomorphological unit, and (3) combining with actual past flood images (during or just after the flood) (Kingma, 2002). This study describes a procedure of small-scale landform classification and flood hazard assessment by the geomorphological approach (see Chapter 2).

1.4 Applications of SRTM, multi spectral/temporal remotely sensed data, and open source software in landform classification and flood hazard mapping

The application of DEMs and satellite images for landform classification in addition to conventional materials (topographic maps and aerial photos) has been increasing for the last several decades to overcome the shortage of data sources in developing countries. Combining Landsat and Shuttle Radar Topographic Mission Digital Elevation Model (SRTM DEM) data is an economical and efficient method for mapping flood hazards and overcoming inadequate data sources in developing countries (Wang et al., 2002). Supervised land cover classifications from Landsat and SRTM DEM data can be combined for assessing coastal flood risk (Demirkesen et al., 2006; Willige, 2007) and digital terrain analysis (Demirkesen, 2008). Three-dimensional (3D) DEM models clearly show the geomorphological relief, which can indicate the characteristics of landforms (Badura and Przybylski, 2005). Shaikh et al. (1989) confirmed the applicability of Landsat Thematic Mapper (TM) for alluvial and coastal landform mapping by visual interpretation associated with field surveys and aerial photos. A variety of alluvial and coastal landforms, such as floodplain features, including natural levees, flood basins, paleo-channels, paleo-meanders, oxbow lakes, and coastal landforms, such as estuaries, tidal flat, lagoons, dunes, and sand bars could

be delineated using this approach. Umitsu et al. (2006) demonstrated the utility of SRTM incorporated with GIS data for studies on flooding and micro-landforms (small-scale landforms). Ground surface height data from SRTM contributes to the investigation of the relationship between flood-affected areas and flood height.

This study aims to classify small-scale landforms on alluvial plains (see Chapter 2, 3, 4) and map flood hazard zones (see Chapter 2) using SRTM and Landsat images and GRASS GIS (Geographical Resources Analysis Support System Geographic Information Systems) software. GRASS is an open-source general-purpose GIS software for the management, image processing, analysis, modeling, and visualization of many kinds of vector and raster data. In particular, 3D visualization using NVIZ function and extruding from 2D to 3D vectors in GRASS can generate 3D diagrams from 2D raster and vector data, which supports interpretation and visualization of data (Hofierka et al., 2008; Neteler et al., 2007). Therefore, this study utilized GRASS as an efficient tool to enhance and support the interpretation and visualization of the data.

The SRTM DEM must be preprocessed before it is used to calculate local land-surface parameters. Preprocessing of the SRTM DEM was generally including (1) filling voids, (2) eliminating the overestimated elevation in the entire low plain, and (3) removing bias from trees and houses.

1.5 Advantages of the digital classification method compared to the manual one for classifying landforms

In the geomorphological approach, geomorphological mapping - landform classification is an important step. It is very crucial to produce landform classification maps precisely, quickly, and objectively. In fact, manual landform classification maps generated by visual interpretation rely on human interpretation (Van Westen, 1993)

although they theoretically have more details and high accuracy. Recently, digital landform classifications, such as automated, semi-automated, and rule-based methods, have been increasingly developed and applied (Bernert et al., 1997; Blankson and Green, 1991; Drăgut and Blaschke, 2006; Drăguţ and Eisanka, 2012; Gallant et al., 2005; Klingseisen et al., 2008; Saadat et al., 2008). The digital approach processes remotely sensed multi-spectral/temporal and digital elevation data. Hence, it is normally more objective, time saving, and convenient to edit digital maps versus manual and visual interpretation using aerial photos and topographic maps. Most previous studies of automated landform classification have been conducted on a large scale (e.g., mountains, plateaus, floodplains) or have focused on mountainous or high-elevation areas where topographical differences are clear and evident (MacMillan et al., 2000; Gallant et al., 2005; Drăgut, & Blaschke, 2006; Iwahashi et al., 2007; Klingseisen, et al., 2008; Saadat et al., 2008). Studies of automated landform classification maps in alluvial plains are scarcer. The possible reason is the relatively low-relief characteristics of alluvial plains. Thus, it is difficult to extract landforms solely by the use of DEMs. Therefore, it is necessary to combine multi-spectral/temporal data such as Landsat and ASTER data that provide supplemental information about land cover when used in combination with DEMs. For the reasons above, this study makes an effort to address the research challenge by proposing a rule-based digital method for automatic mapping of small-scale landforms in an alluvial plain using the SRTM DEM with multi-spectra/ temporal remotely sensed data (see Chapter 3). Moreover, floodplains formed by large rivers such as Red River and Mekong River are too large to make manual landform classification maps by visual interpretation. Therefore, the digital rule-based landform classification method has more essential role in those cases. The integrated utility of land cover characteristics from multi-spectral/temporal remotely sensed data, local

land-surface parameters from the SRTM DEM, and relative position analysis to classify landforms in a flat alluvial plain demonstrated the significance of these factors in the landform classification of alluvial plains.

However, these inputs, especially local land-surface parameters, are not always consistent in different areas due to topographic characteristics, despite similar study objectives (e.g., Hammond, 1954; Gallant et al., 2005; Drăguţ and Eisanka, 2012). In other cases, classification schemes are adjusted to local situations and research objectives (e.g., Verhagen and Drăguţ, 2012). Therefore, the next part of this study describes adjustments to the rule-based digital landform classification method proposed by Ho et al. (2012) (presented in Chapter 3) for a case study on the western plain of the Red River delta, northern Vietnam, for the evaluation of flood susceptibility (see Chapter 4).

1.6 Research questions

To address the research issues mentioned above, this thesis must answer the following questions:

1. How to employ available data (SRTM DEM and Landsat images) for small-scale landform classification and flood hazard zonation in regions where detailed topographic and land cover data are insufficient? (see Chapter 2)
2. How to produce landform classification by a rule-based digital method using SRTM DEM and multi-spectral/temporal remotely sensed data to facilitate the manual landform classification procedure that is often known as time-consuming, subjective, and difficult to edit? (see Chapter 3)
3. Is this method applicable for other alluvial floodplains and how to generalize this method for wide applications? (see Chapter 4)

1.7 Thesis outline

Chapter 2 presents the overarching procedure of flood hazard assessment by a geomorphological approach. Small-scale landform classification was developed using an integrated method utilizing Shuttle Radar Topographic Mission (SRTM) and Landsat ETM+ (Enhanced Thematic Mapper Plus) data combined with field investigation. Then, a flood hazard zonation map was generated by categorizing geomorphological features and the average elevation of each landform into flood hazard classes. The results were validated using field surveys, topographic maps and past inundation images. The case study is the Thu Bon alluvial plain, central Vietnam.

Chapter 3 concentrates on the development of a rule-based digital method for generating a landform classification map of the alluvial plain in central Vietnam (the study area same as that in Chapter 2) by using thresholds of the Modified Normalized Difference Water Index (MNDWI), land cover characteristics, local relief, average elevation, channel features, and relative position indices.

Chapter 4 reports adjustments to the rule-based landform classification method proposed by Ho et al. (2012) (in Chapter 3) for a case study on the western plain of the Red River delta, northern Vietnam with an attempt to generalize the rule-based digital method to other floodplains.

Chapter 5 concludes the effectiveness of the landform classification (either manual or rule-based digital methods) for flood hazard assessment using SRTM DEM and multi-spectral/temporal remotely sensed data. In particular, it affirms the advantages of the rule-based digital method compared to the manual one, and the possibility to generalize the rule-based method for wider applications.

CHAPTER 2 – Landform classification in small scale and flood hazard assessment of the Thu Bon alluvial plain, central Vietnam via an integrated method utilizing remotely sensed data

2.1 Introduction

The coastal alluvial plains in central Vietnam are vulnerable to flooding due to high rainfall, narrow coastal plain, short steep rivers, and high population density due to good living conditions in these areas. Therefore, plains in this part have more inundation potential by not only flooding but also sea-level rise. Furthermore, flood damages depend greatly on settlement patterns, land-use decisions, and the quality of flood forecasting, warning and prevention systems. In addition, human encroachments on floodplains with shortage of flood response plans increase the damage potential. For this reason, flood hazard mapping in relation to geomorphic features, particularly in alluvial plain, has played an important role in forecasting, and managing flood hazard in many regions of the world. Generating a conventional landform classification map uses aerial photos and topography map as the first choice. However, in fact, developing countries have been facing with the state of insufficient and inconsistent data, particularly topographic and land-cover data. Therefore, utilizing satellite images, especially open available data (Landsat and SRTM DEMs) can help to solve that problem in developing countries where data cost has become a significant obstacle for researches. Landsat data have been the most popular remote sensing data and used for land cover analysis since the beginning time of satellite image application. Up to date, this kind of spectral images has never declined their valuable role in studies of geosciences, especially in developing countries because of their open availability. In

addition, topographic data sources are limited and difficult to obtain in developing countries where funding for purchasing high quality materials is limited. SRTM DEMs, available from February 2000 with 80% landmass, have proved huge applications on geosciences, particularly geomorphology and hydrology (NASA/JPL).

Flood susceptibility mapping using geomorphological approaches is effective for delineating flood extent and various degrees of potential flood-affected areas. This approach is useful where the channel system and floodplain morphology change dynamically and in regions where detailed DEMs are not available.

This chapter presents an integrated method for classifying small-scale landforms in relation to flood inundation by visual interpretation. The "small-scale" term in this study indicates spatial extent (size of the area and landform features) but spatial resolution. This manual method used the 90-m-resolution Shuttle Radar Topographic Mission Digital Elevation Model (SRTM DEM) and Landsat Enhanced Thematic Mapper Plus (ETM+) data. Landform units of an alluvial plain were classified by integrating elevation and landforms derived from the SRTM DEM with spectral characteristics derived from a pair of Landsat images of dry and flood seasons. Then, a method for flood hazard zonation based on the geomorphological approach was developed. Three-dimensional (3D) diagrams of the composed maps were produced using Geographic Resources Analysis Support System (GRASS) 6.3 to visualize the geomorphological features and flood hazard levels. The results were validated by field investigation, aerial photos, topographic maps, and images of past inundation. The results revealed a close relationship between the geomorphological characteristics and flood conditions of the region. Flooding and sedimentation mechanisms create dynamic fluvial and coastal landforms, and these geomorphological features, in turn, affect the

flood hazard potential. The landform classification map can be used to effectively predict the extent of flood hazard potential (Ho and Umitsu, 2011).

2.2 Study area

The Thu Bon alluvial plain is formed by the Thu Bon River and the Vu Gia River (Fig. 5). The Thu Bon River, which is approximately 205 km in length, originates from Ngoc Linh Mountain (2,598 m) in the Truong Son range in Kon Tum province and then flows through a portion of Quang Ngai province and most of Quang Nam province in central Vietnam. It first runs south, changes its course to a northeasterly direction and finally flows east down to the Thu Bon alluvial plain, where it drains into the South China Sea via the Dai River. The Thu Bon River lacks a distinct alluvial fan (Kubo, 2002). The river channel exhibits a braided and/or anastomosing pattern, which is associated with meandering and anabranching. The alluvial plain is not only governed by fluvial processes due to frequent flooding but also by coastal processes, such as wave, longshore or/and aeolian processes. Therefore, the plain is dominated by levees, meanders, channel bars, and flood basins in inland areas and by sand dunes in the coastal zone.

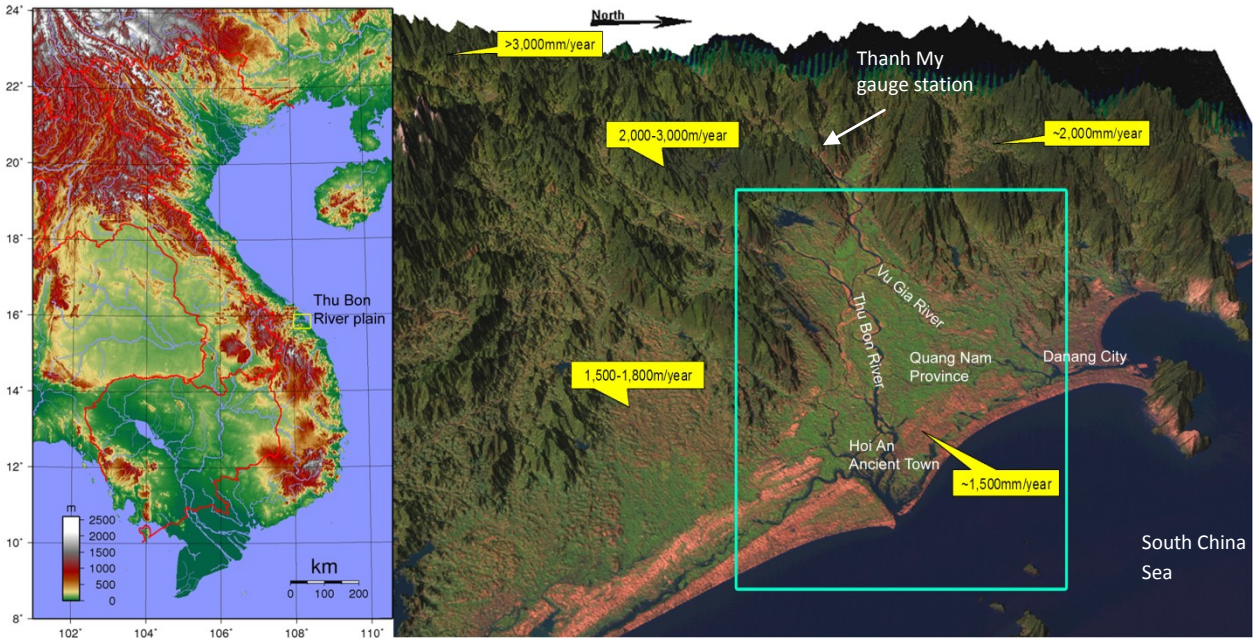

Fig. 5. Study area of the Thu Bon River plain in central Vietnam and rainfall distribution.

Sandy sediment dominates the river load and also governs the flow mechanisms and drainage of the river. The bed load of the Vu Gia-Thu Bon basin has increased over the last century due to upstream deforestation resulting in unconsolidated soil, as well as exploitation of high slopes for settlement and cultivation (Centre for Hydro-meteorology Quang Nam, 2001). The average volume of the sediment supply measured at Thanh My gauge station on the Vu Gia River is 460,000 tons per year. Consequently, the delta front is progressively elevated and shifted seaward by sediment deposition, and flood levels have tended to be increasing in recent years (Fig. 6) (CCFSC, 2006; Nguyen, 2007).

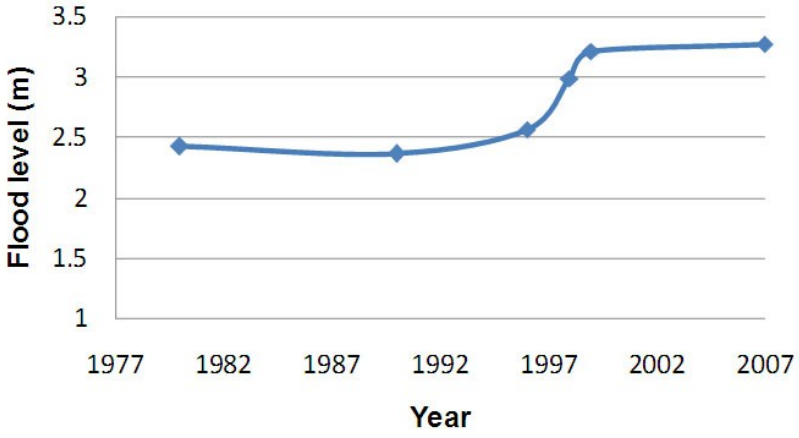

Fig. 6. The increasing trend of flood levels at the Hoi An gauge station from 1980 to 2007.

This alluvial plain in the central part of Vietnam is characterized by the highest rainfall in the country. The rainy season spans from September to December. The average annual rainfall in upland areas of the basin is approximately 3,000-4,000 mm, which is much higher than in coastal areas (approximately 2,000 mm per year). Approximately 60-76 % (75-76 % in coastal areas) of the annual rainfall is received in the rainy season and results from storms and typhoons that cause flooding. The major flood events that occurred in this area in 1964, 1999, 2007, and 2009 were caused by complex meteorological phenomena (storms, typhoons, and tropical low pressure) causing torrential rain in most provinces in the central and southern regions of central Vietnam.

In general, most areas of Quang Nam province and the Vu Gia–Thu Bon alluvial plain are rural, with agriculture as the primary economic activity. The problems of flood damage in Thu Bon plain and the town of Hoi An are usually associated with local social and human activities in the low-lying areas. Local people have settled in

areas vulnerable to flood damage because of the convenience of such areas for their livelihood and customs (Quang Nam CFSC, 2009).

2.3 Data sources and processing

2.3.1 SRTM DEM characteristics and processing

The Shuttle Radar Topography Mission (SRTM) successfully collected Interferometric Synthetic Aperture Radar (IFSAR) data covering 80 % of the landmass of the Earth between 60º N and 56º S. It collected the first ever high-resolution near-global digital elevation data (Zandbergen, 2008).

The SRTM data used in this study were WRS (World Reference System) tile SRTM 3 arc-second (90 m resolution) set up in path-row size and matched with LANDSAT locations and measurements with file format GeoTIFF and path 124-row 049.

Filling voids

Prior to using SRTM data, substantial pre-processing operations are required. Voids in SRTM data commonly appear in high elevation areas and in areas such as water surfaces and sandy areas. These voids are due to shadow and layover effects, especially in mountainous areas, which cause a poor signal return to the sensor, and to smooth areas, such as water or sand, which scatter too little energy back to the radar system (Rodriguez, 2005 and 2006; Zandbergen, 2008).

The SRTM DEM used in this study was the finished SRTM DTED (Digital Terrain Elevation Data) Level 2. Although it has been edited based on the SRTM Edit Rules following several processes, such as defining water bodies and coastlines and filling voids (spikes and wells), some data are still missing (Zandbergen, 2008). There are several techniques and programs available to fill-in missing data (Kuuskivi et al., 2005;

Reuter et al., 2007). In this study, 3DEM software was adopted to patch spikes and wells.

Adjusting overestimated elevations from SRTM DEM

The DEM obtained from SRTM data is not a "bare-earth" surface or a Digital Terrain Model (DTM) but, rather, a Digital Surface Model (DSM), in which land is covered by a tree canopy and/or buildings known as noise. Thus, the land surface height is only reflected in areas that are not covered with high vegetation or buildings (Koch et al., 2000; Guth, 2006). SRTM typically overestimates elevation values at low elevations (less than 2,000 m) and underestimates them at higher elevations (Berthier et al., 2006). Therefore, the SRTM DEM data were adjusted using an offset to match the real elevation of the terrain because this study area is located at low elevations.

To calculate this offset, 55 points were selected at random for comparison of the SRTM DEM elevation using 1:25,000 topographic maps for the reference elevation (Fig. 7). The points used for elevation comparison were in bare, sparse or low vegetation areas, such as paddy fields or bare soil areas. The vertical root mean square error (RMSE) between the SRTM DEM value and the real elevation was calculated by the modified RMSE formula of Li (1988), as follows:

$$\mathrm{RMSE} = \sqrt{\frac{\sum_{i=1}^{n}\left[z_{(\mathrm{SRTM})} - z_{\mathrm{REF(topomap)}}\right]^2}{n}} \qquad (1)$$

where $z_{(\mathrm{SRTM})}$ is the elevation of the point, and $z_{\mathrm{REF(topomap)}}$ is the reference elevation of the same point from the topographic map. The resulting vertical RMSE value was approximately 3.5 m for this area. SRTM data have absolute and relative height errors of 6.2 and 8.7 m, respectively, in Eurasia (Rodríguez et al., 2005 and 2006), therefore this RMSE value was considered acceptable. The correction to remove

the vertical RMSE from the SRTM DEM data was implemented using the command r.mapcalc in GRASS 6.3 (Neteler et al., 2007).

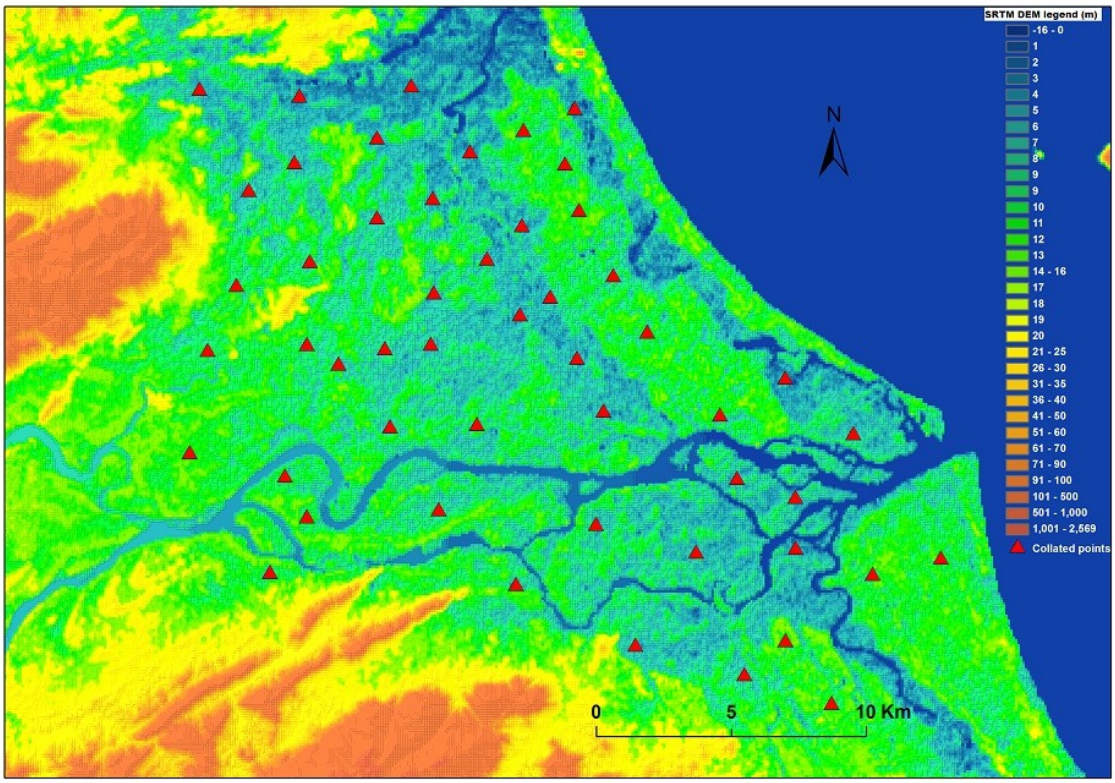

Fig. 7. Location of the 55 points (indicated with triangles) selected to calculate the vertical RMSE between the SRTM DEM data and topographic maps.

2.3.2 Landsat dataset characteristics and processing

The resolution of Landsat images is 30 m in bands 1-5 and 7 (visible, near infrared and short wave infrared); 60 m in band 6 (thermal infrared) and 15 m in band 8 (panchromatic). A pair of Landsat Enhanced Thematic Mapper Plus (ETM+) images from March 23, 2001, in the dry season and October 17, 2001, in the flood (rainy) season (path 124/row 48), were selected to identify land cover characteristics in the study area. These images were in the GeoTIFF format, with the WGS84 ellipsoid datum and the Universal Transverse Mercator (UTM) coordinate system for zone 49N.

Composites of these Landsat images were created with False Color Composite (FCC) RGB 542. These composite images were then pan-sharpened by image fusion using band 8 (panchromatic) to enhance the spatial resolution of the composite images from 30 to 15 m.

2.4 Methodology

2.4.1 Mapping small-scale landforms using LANDSAT images and SRTM DEM

Alluvial plains are characterized by low relief and are formed by frequent and active deposition, aggradation from channelized, and overbank flows (Allen, 1965; Speight, 1974). Therefore, their small-scale landforms are composed of primary landform types (floodplain, bar plain, meander plain, stagnant alluvial plain, delta, and terraces), together with primary morphological elements (stream channels, bars, channel fill, alluvial islands, natural levees, and flood basins).

The small-scale landform categories of the Thu Bon plain can be classified into mountains and hills (which define the boundaries of the plain), terraces (higher, middle, and lower), valley plains, flood basins, natural levees, deltaic lowland, former river channel, dry river bed, inter-dune marsh or swale, sand dunes, and permanent water.

In this study, these small-scale landforms were categorized by visual interpretation of SRTM DEM micro-relief and land surface features from LANDSAT images (Umitsu et al., 2006). The SRTM DEM micro-relief displayed using the NVIZ 3D visualization tool of GRASS 6.3 can be significantly accentuated to facilitate the detection of the relief. The small-scale landforms can also be delineated by characteristics of the land surface indicated in the LANDSAT images. However, suitable LANDSAT data should be selected for the identification of the pattern and shape of various small-scale

landforms. Comparison of the dry and flood season LANDSAT images reveals the land cover characteristics of the alluvial plain and the relationship between land cover and small-scale landform elements. The October image (taken after the harvest, without crop coverage) reveals remarkable flood basin and valley plain areas (normally paddy fields), as well as typical elongated forms of natural levees distributed along the river side or former river channel. In particular, the texture of the levees could be identified well because the land cover on levees in rural areas in Vietnam is generally a mix of houses and trees. In SRTM DEM, natural levees can be identified as elevated edges at the corresponding positions.

The two LANDSAT ETM+ images and the SRTM DEM were co-registered using the rectify function in ArcGIS 9.2 to make them fit to each other with an error of 0.3 pixels. The SRTM DEM has 1-m height intervals. The process of digitizing landform units was performed in both ArcGIS and GRASS 6.3. LANDSAT images were overlaid on the SRTM DEM to carry out digitizing. A 3D diagram of the SRTM DEM generated by NVIZ in GRASS GIS could be used to identify landforms (Fig. 8).

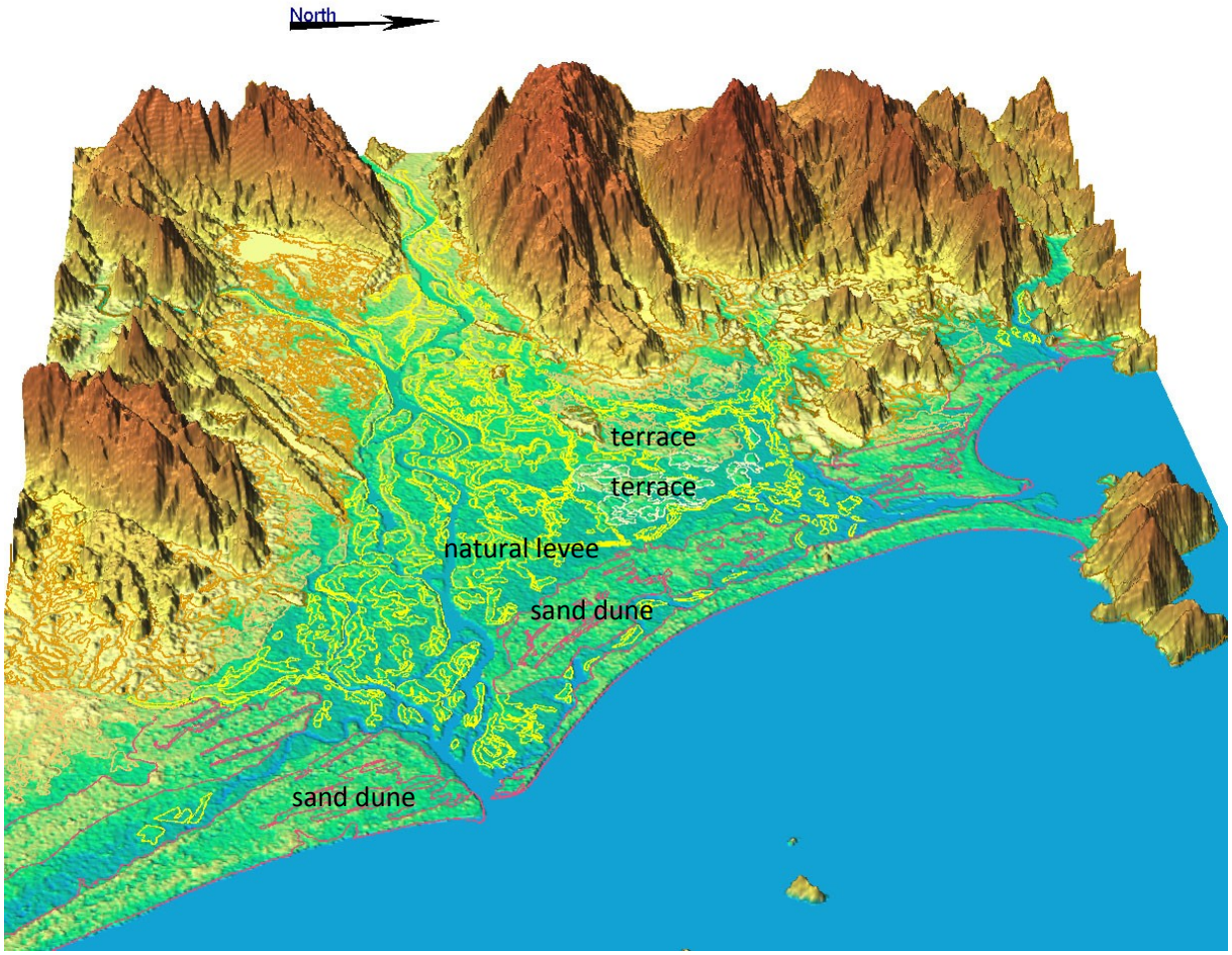

Fig. 8. The 3D diagram of the SRTM DEM with terrain relief classified into various small-scale landforms on the Thu Bon alluvial plain.

Flood basins were classified using [band 4 - band 3] of the October LANDSAT image (ETM4 - ETM3). The LANDSAT image from October 17, 2001, was taken before the flood event of October 19-22, 2001, which was caused by tropical low pressure. Despite flood conditions not being present in this image, the persistent rainfall in this season means that the soil contains a high amount of water. Therefore, areas with high moisture, indicating lowland areas and flood basins, could easily be identified in the October image. In this area, ETM4 - ETM3 was effective for the identification of moist surfaces because ETM4 is the best band for the detection of water and for

distinguishing water from land while ETM3 has high reflectance for most soils (Biradar et al., 2003). Fig. 9 shows that low values of ETM4-ETM3 give a good indication of moist soil areas.

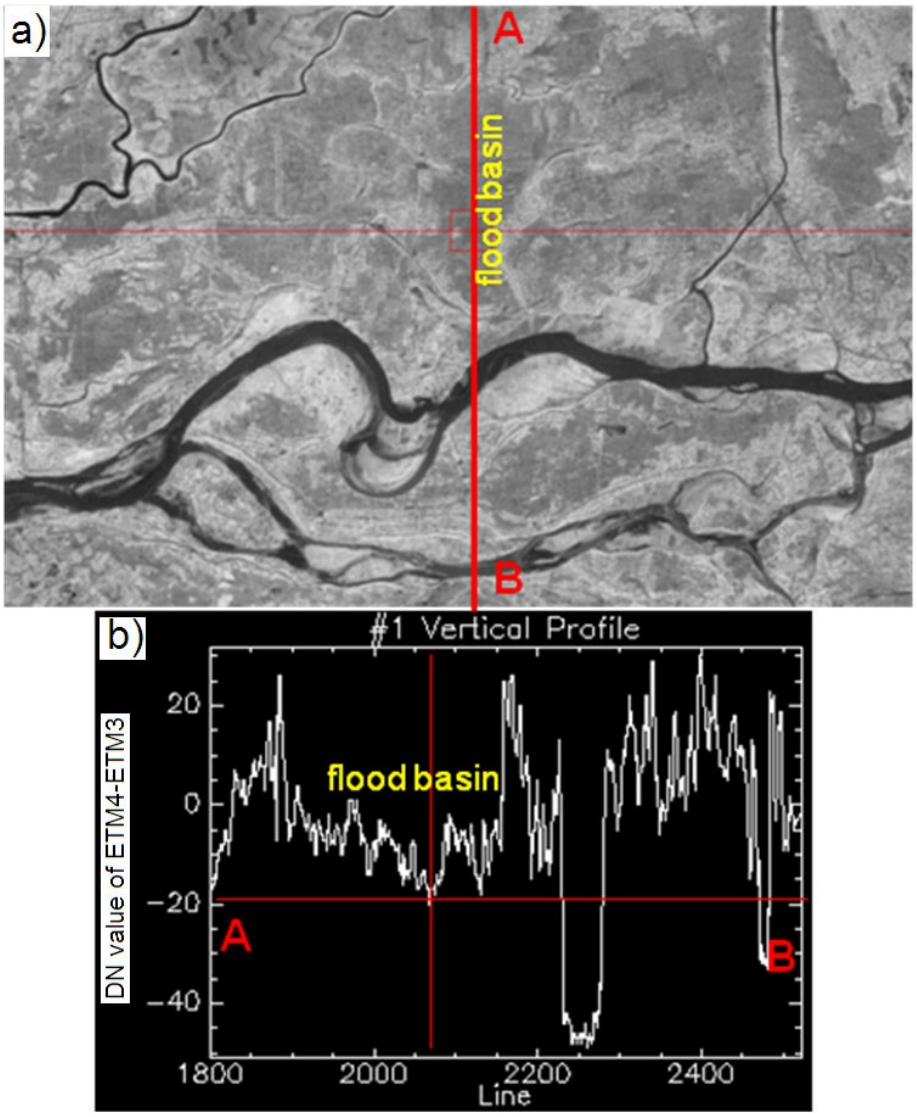

Fig. 9. Low values of ETM4-ETM3 indicate high moisture areas (flood basin and lowland). (a) shows a sample of flood basin areas, and (b) shows cross-section AB, as indicated in (a).

Water surfaces, mountains and hills were identified as the boundaries of the alluvial plain. Sand dunes were identified in the SRTM by their typical elongated shape aligned with the coastline and their prominent relief in this relatively low area (Blumberg, 2006). The tone of sand dune land cover is bright and is almost the same in both LANDSAT images. The overestimation of elevation in the SRTM data in low relief areas (Guth, 2006) is an advantage in the visual interpretation of these data based on relief characteristics.

In dry river beds, point bars exhibit a tone similar to that of sand dunes; however, they differ in shape and position. They commonly form at growing meanders of rivers (Melton, 1936) and in river beds during the dry season when there is no water flow. Former river channels can be delineated in the October LANDSAT image. At the time the data were obtained, the old channels were fed by rain water, thus they appear as discontinuous river channels in the non-cropped image.

Terraces have the same texture as natural levees in LANDSAT images, but they differ from natural levees in their shape and elevation. There are three levels of terraces: higher (9-12 m), middle (7-8 m), and lower (4-6 m).

The deltaic lowland areas, also known as lower flood basin areas, are located in the estuarine area have low elevations in the SRTM DEM (< 3 m) and a high moisture content in the SRTM DEM and the October 17 LANDSAT image. Thus, deltaic lowland areas were placed in a different category from flood basin areas.

2.4.2 Flood hazard zoning

In this study, the geomorphological characteristics, flood characteristics, and the average ground elevation of each landform were used to analyze and categorize flood hazard zones. The flood heights determined from field surveys and past flood maps

obtained from MODIS in 2006 and 2009 were used to check the accuracy of the flood-affected areas.

Geomorphological features reflect the characteristics of flood inundation (Baker et al., 1988; Oya, 2002), and the elevation of an alluvial plain generally increases inland. Therefore, despite similar elevations, the flood states of certain areas are not coincident. For instance, in the case of a flood basin and a natural levee, although the height of natural levee 1 (Z1) is the same as that of flood basin 2 (Z2), the flood level of natural levee 1 (h1) is lower than that of flood basin 2 (h2) because the flood surface is inclined (Fig. 10). We found that the level of flood hazard in the same landform category was not constant over the whole area due to the gradient of the terrain and the flood water surface. Therefore, ground elevation was considered a supplementary indicator for flood hazard classification.

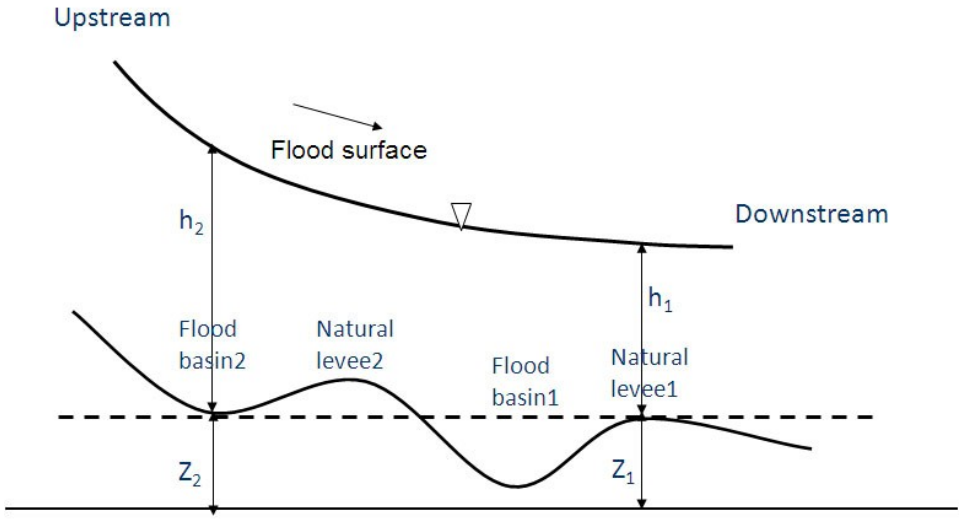

Fig. 10. Model showing the different flood levels of a natural levee and a flood basin at the same elevation.

Because SRTM DEMs are characterized by speckling noise due to the effect of land cover (Zandbergen, 2008), particularly in areas of low slopes, it is necessary to

standardize SRTM elevation data by converting the elevations into average elevations. The average elevation of each landform object was calculated by applying the r.average command in GRASS (Neteler et al., 2007) (Fig. 11). Thus, the landform features could be re-checked based on their average elevation, and those in incorrect categories could be reassigned.

The flood hazard zone classification employed here is explained in Fig. 12 and Table 1. Then, a 3D diagram of the flood hazard map was generated by overlaying the classification on the SRTM DEM.

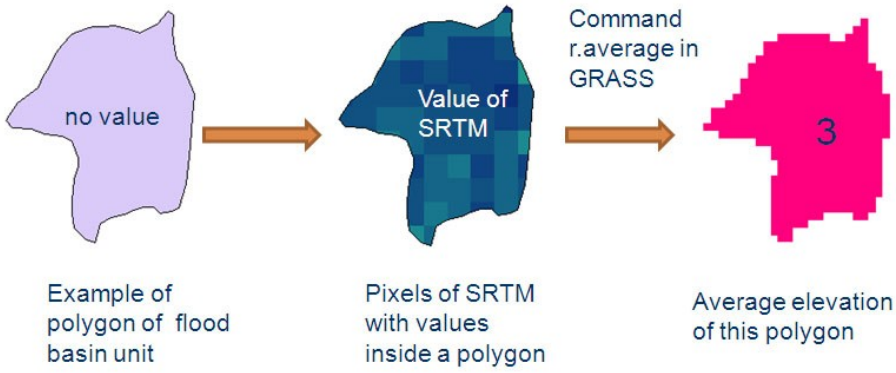

Fig. 11. The process of average elevation calculation.

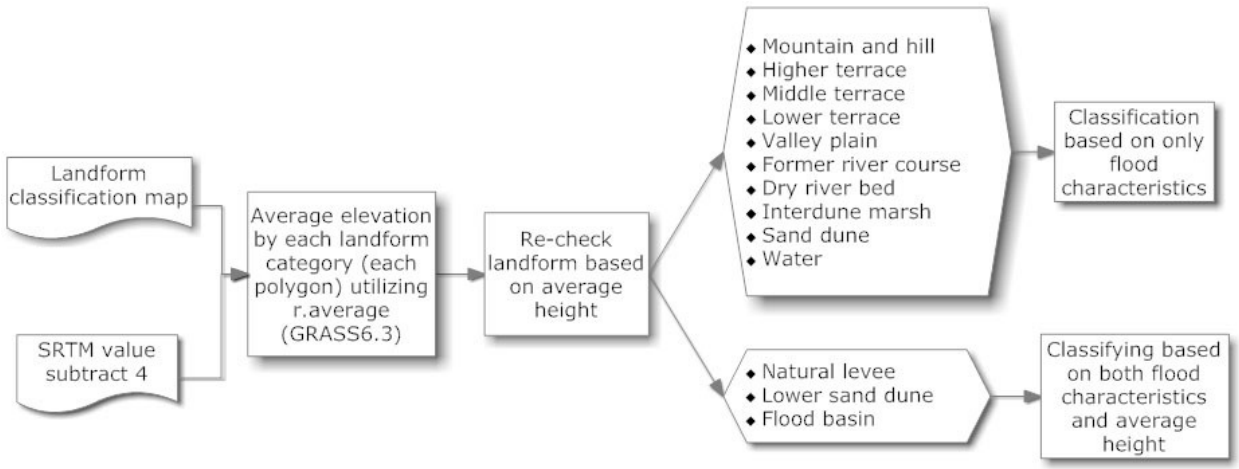

Fig. 12. The process of flood hazard mapping used in this study.

Table 1. Degree of flood hazard classification.

ID	Geomorphological unit	State of flooding	Average elevation	Flood hazard class
1	Mountain and hill	Unsubmerged		No hazard
2	Higher terrace			
3	Middle terrace			
4	Sand dune			
5	Interdune marsh	Submerged during torrential rainfall		Moderate
6	Lower terrace	Submerged in major flood		Low
7	Valley plain (VP)	When submerged, high velocity of current but drains well	VP in mountain and hill	High hazard of flash flood
			VP of terrace in plain	High
8	Natural levee	Submerged during extraordinary floods but drains well	< 3m	High
			3 m – 4 m	Moderate
9	Lower sand dune		4 m – 6 m	Low
			> 6m	Very low
10	Former river channel	Submerged for long period, deep water		Very high
11	Dry river bed			Very high
12	Deltaic lowland			Very high
13	Flood basin		<3m	Very high
			3m – 6m	High
			>6m	High hazard of flash flood

2.5 Results and discussion

2.5.1 Landform and small-scale landform characteristics in relation to flood conditions

Figure 13 shows the landform classification map for three parts of the Thu Bon alluvial plain in terms of flood inundation characteristics. The landform classification map is displayed in a 3D diagram to better view the landforms.

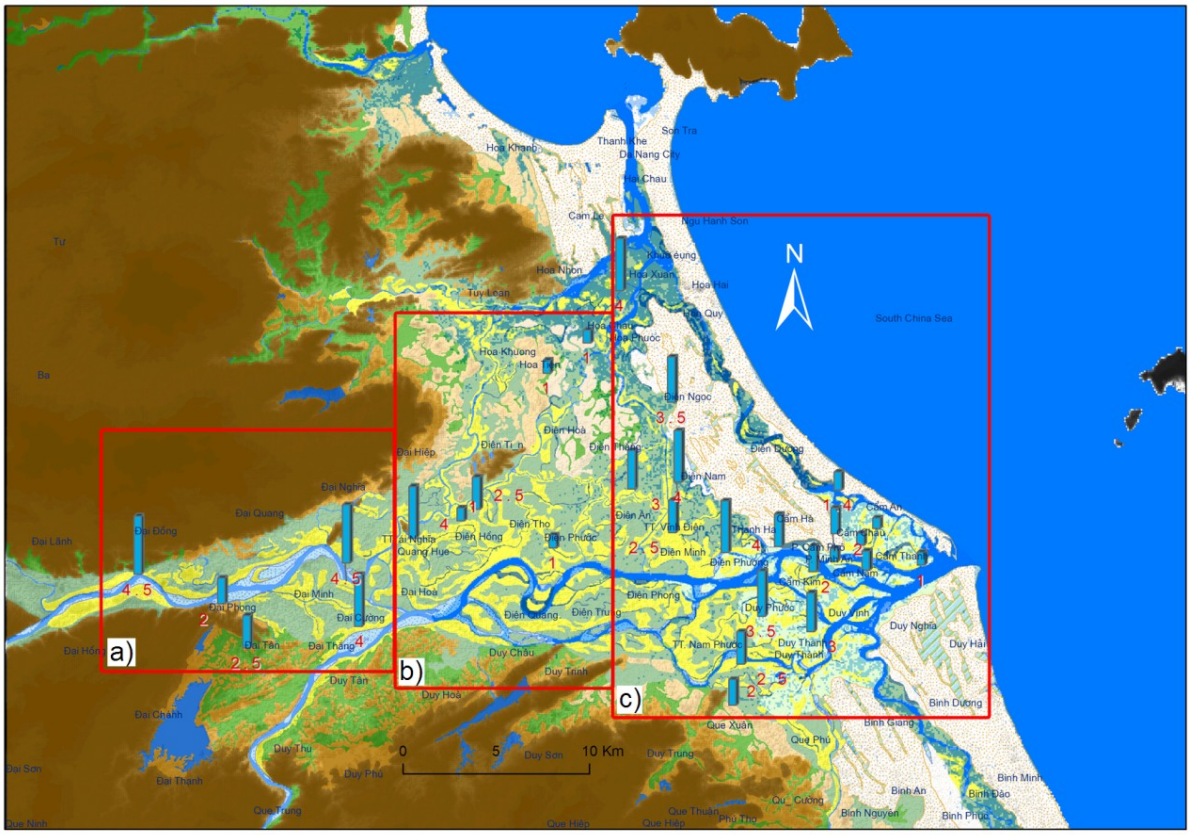

Legend

- Mountain_and_hill
- Higher_terrace
- Middle_terrace
- Lower_terrace
- Valley_plain
- Natural_levee
- Flood_basin
- Deltaic_low_land
- Former_river_course
- Dry_river_bed
- Inter-dune_marsh
- Sand_dune
- Lower_sand_dune
- Water
- Hmax flood 1999

North

d)

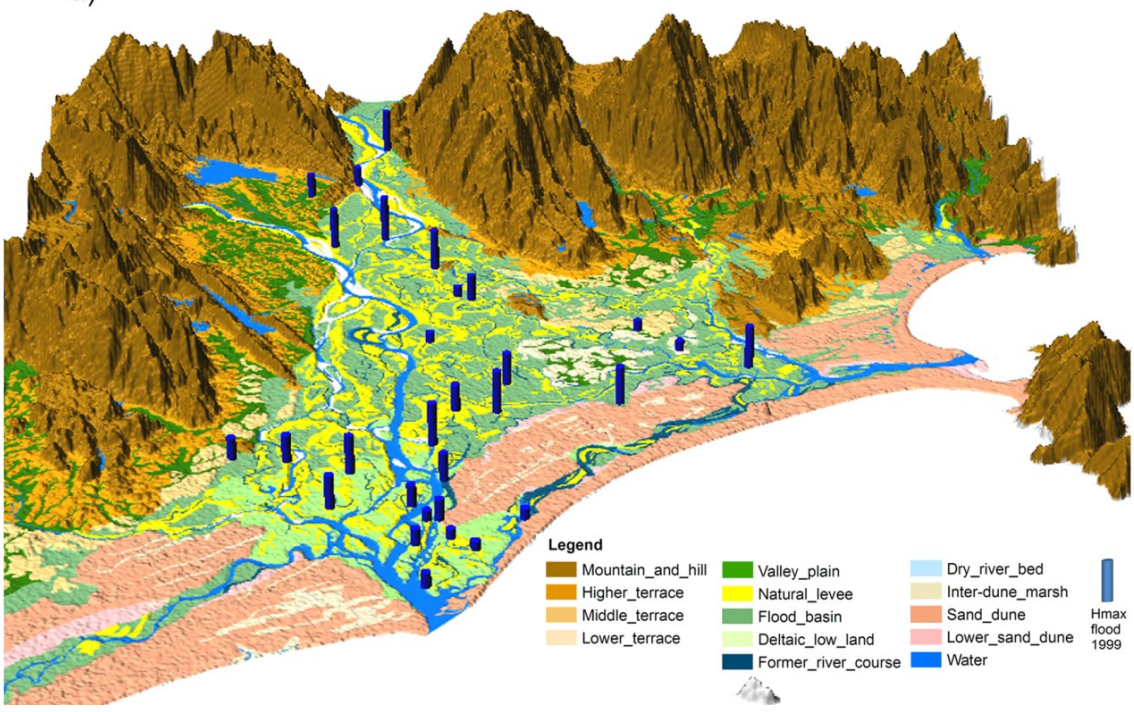

Fig. 13. Landform classification map of the Thu Bon alluvial plain, with flood depths as measured through field surveys: (a) around the confluence of the Vu Gia and Thu Bon rivers, (b) the middle of the Thu Bon River floodplain and (c) estuary of the Thu Bon River. The columns indicate the highest flood depth in the flood event of 1999, with the values given. The image (d) shows 3D diagram of the landform classification map of the Thu Bon alluvial plain.

Mountains and hills occur west of the Thu Bon alluvial plain. Terraces are dominant north of the Thu Bon River as a result of interactions of the sediment of the Vu Gia-Thu Bon river system. In the alluvial plain, terraces are characterized as elevated regions among surrounding large lowlands.

Valley plains are located in the mountainous and hilly areas, and are the floors of valleys. They also develop on the surface of terraces. Flood conditions in valley plains are characterized by flash floods and relatively short periods of inundation.

In the floodplain, the channel pattern of the Thu Bon River is described as braided or anastomosing. Braided channel patterns, which are associated with alluvial islands and channel bars, occur in many rivers with steep slopes and relatively coarse bed materials (Melton, 1936). Small-scale landforms of floodplains include natural levees, flood basins, dry river beds, and former river channels.

Natural levees are the result of overbank flood sediment deposition and play a critical role in revealing the mechanisms of past flood inundation. Natural levees are the highest elevation component of floodplain topography (Allen, 1965). The floodplain formed by the Vu Gia-Thu Bon river system extends broadly from the Thu Bon river course in the west-east direction.

Dry river beds and channel bars are well developed in branches of the Thu Bon River and the Vu Gia River in the area of Dai Phong district. Dry river bed areas are the accretion regions of growing meanders (Melton, 1936); they are good indicators of the large alluvial sediment supply in this river system. Observation of these areas in the dry season reflects the significant decline in river discharge at that time.

Flood basins (back swamp) are the lowest parts of a floodplain (Allen, 1965). Flood basins are flat and relatively featureless areas with little or no relief and poor drainage capacity. The sediment of flood basins is commonly muddy, with suspended fine sediments being left after coarser suspended sediments are deposited on levees in overbank flows. In the Thu Bon alluvial plain, most flood basins are used as paddy fields or for other agricultural activities because of their fine sediment and water-preserving characteristics. Flood basins normally occur between two channels where coarser sediment is held in adjoining natural levees (Allen, 1965). The main channel of the Vu Gia-Thu Bon River system extends broadly from west to east, and flood basins also exist between the main river channel and its tributaries.

Former river channels are another typical geomorphological feature of this alluvial plain that arise due to significant changes in the river's course over time. A large former river channel on the Thu Bon alluvial plain is located in the Thanh Ha district in the western part of Hoi An city at the southern edge of a sand dune where severe flooding occurs nearly every year. Another former river channel that connected the Thu Bon River and the Han River in the past is situated between sand dunes; it now consists of elongated ponds. Many former river channels are located in paddy fields, but evidence of their existence has been removed to some degree by intensive agricultural activities (Nguyen, 2007).

Deltaic lowland is the type of lowland situated in the estuarine areas of the Thu Bon River and the Han River (the Vu Gia river) at Da Nang city.

Sand dunes in the Thu Bon alluvial plain consist of rows of sand dunes aligned parallel to the coastline. These sand dunes block river flood waters from the estuarine area coursing into the river mouth and entering the South China Sea. Between the sand dunes, there are typically inter-dune marsh areas lower than the adjacent dune surface, which can be inundated by ground water and rain.

2.5.2 Flood conditions and their interaction with geomorphological features

Flood conditions around the confluence of the Vu Gia and Thu Bon Rivers (Fig. 13a)

The flood mechanism and small-scale landforms in this region are governed and formed by two rivers. Due to a lack of embankments, shallow river beds and poor drainage capacity, the flood water overflows and inundates the entire lowland plain region, including parts of the following districts: Dai Loc, Dien Ban, Duy Xuyen and Hoi An city (Quang Nam CFSC, 2009).

Flood conditions in the middle of the Thu Bon River floodplain (Fig. 13b)

In less severe flood events, such as the flood of 2006 that was due to Typhoon Xangsane, flood water inundates lowlands that are mainly classified as areas such as flood basins (paddy field) and former river courses. Natural levees are usually affected by overbank flows. However, in major floods, such as those that occurred in 1999 and 2007, flood water covers most areas of the Vu Gia-Thu Bon alluvial plain, except for higher areas. The flood inundation depths on a natural levee were approximately 1 m, compared to 2.5 m in the adjacent lowland. In particular, although a part of the Vu Gia River flow is split at the Quang Hue connector and distributed into the channel of the

Thu Bon River, the Thu Bon River returns water to the Vu Gia River through the Vinh Dien canal in the Dien Ban district, and water collects in the mouth of the Han River at Da Nang city. As a result, the lowland area of southern Da Nang city can become submerged to a high inundation depth of approximately 4 m.

Flood conditions in the Thu Bon river estuary (Fig. 13c)

Although the flood depth is not high (approx. 1 m) in the estuarine area, flood water can cover a large portion of this area. The river bed is aggraded due to intensive deposition of sediment from upstream. In particular, a large sunken sand bar is present at the delta front, which blocks water drainage and causes flood water to stagnate and most of the deltaic lowland to be submerged in the flood season. However, the flood inundation conditions of this area differ on either side of the sand dunes on the two sides of the mouth of the Thu Bon River. These sand dunes act as two bars narrowing the outlet of the river (Fig. 14). Thus, flood inundation on the western side of the sand dunes (2-3.5 m) is deeper than on the eastern side (less than 1.5 m), where flood water drains more readily into the South China Sea.

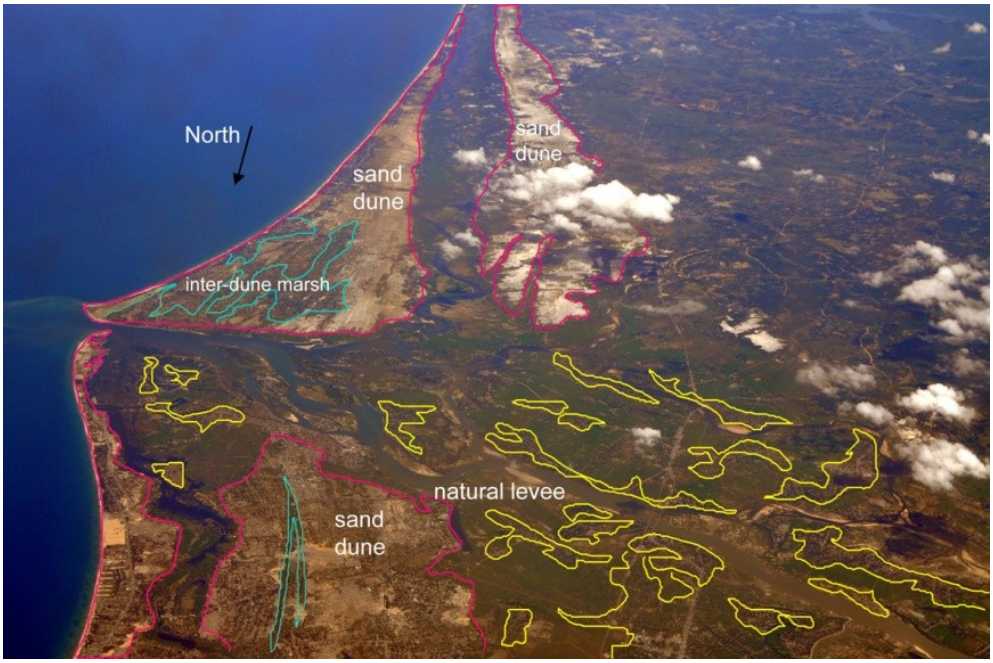

Fig. 14. An aerial photo (June 24, 2009) showing the distinctive sand dune and sand bar system at the river mouth as well as the natural levees along the Thu Bon River (photo by M. Umitsu).

2.5.3 Flood hazard zone analyses

The flood hazard map (Fig. 15) reveals that much of the Thu Bon alluvial plain is at high flood risk or is a flash flood hazard (43.34% area). A vast portion of the lowlands (ground elevation lower than 3 m) is located near the river mouth and in the coastal zone, and experiences frequent and deep inundation. The flood depth ranges from 0.5 m, in estuarine districts of Hoi An city to approximately 4 m around southern Da Nang city.

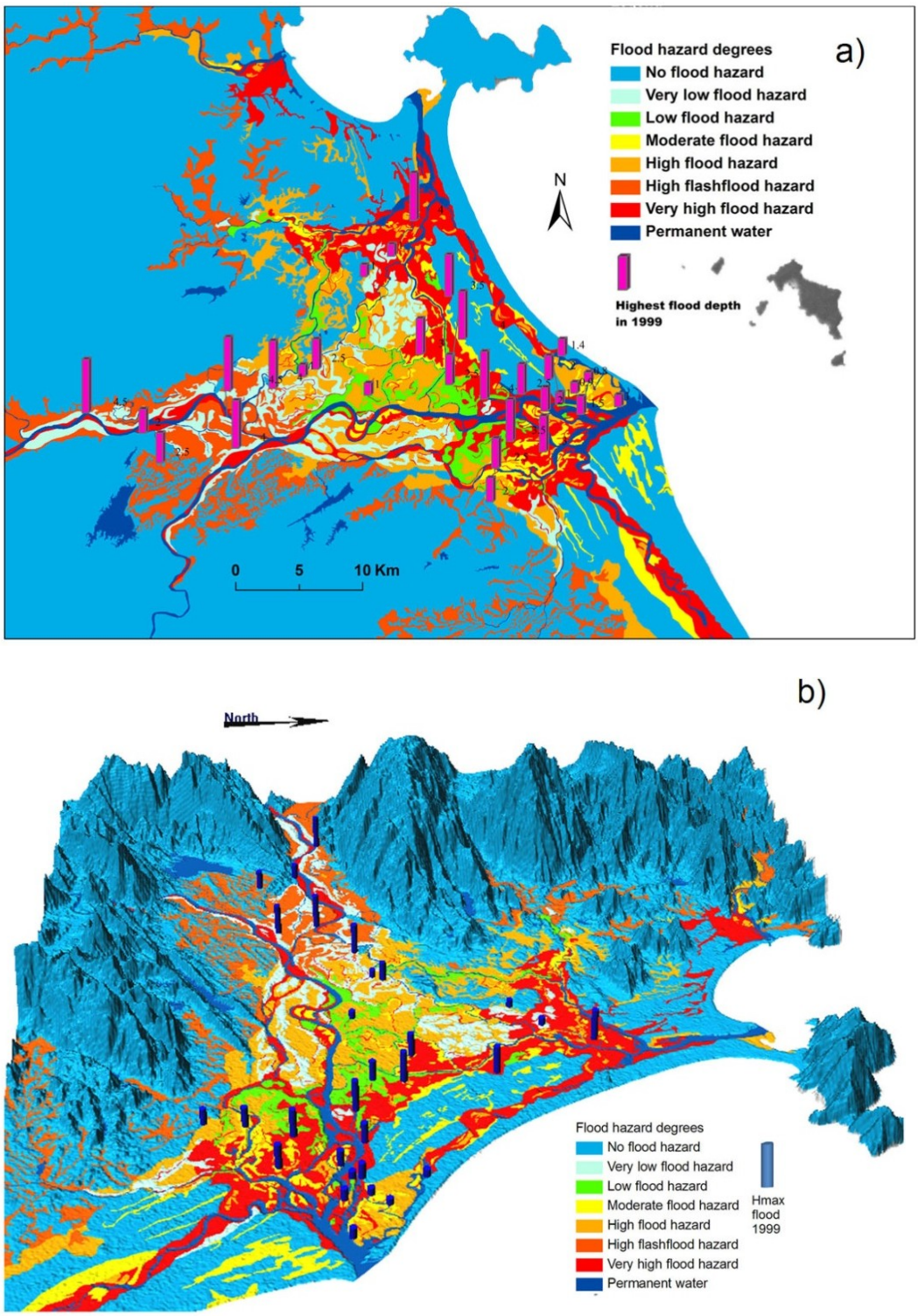

Fig. 15. (a) Flood hazard map and flood height, as determined by field surveys of the Thu Bon alluvial plain and (b) 3D diagram of the flood hazard map of the Thu Bon alluvial plain.

The very high and high hazard areas in the plain correspond well with the areas that experienced a high flood level (2-4 m) in 1999 and were submerged both in the major flood of September, 2009 due to Typhoon Ketsana (rainfall approx. 914 mm) and in the normal flood event of 2006 due to Typhoon Xangsane (rainfall 200-300 mm) (http://www.reliefweb.int/rw/rwb.nsf/db900SID/JBRN-7WLDXF?OpenDocument, accessed on December 2, 2009). The very low and low hazard areas also coincide well with the non-inundated areas shown in flood inundation maps created from MODIS in 2006 and 2009 (Fig. 16).

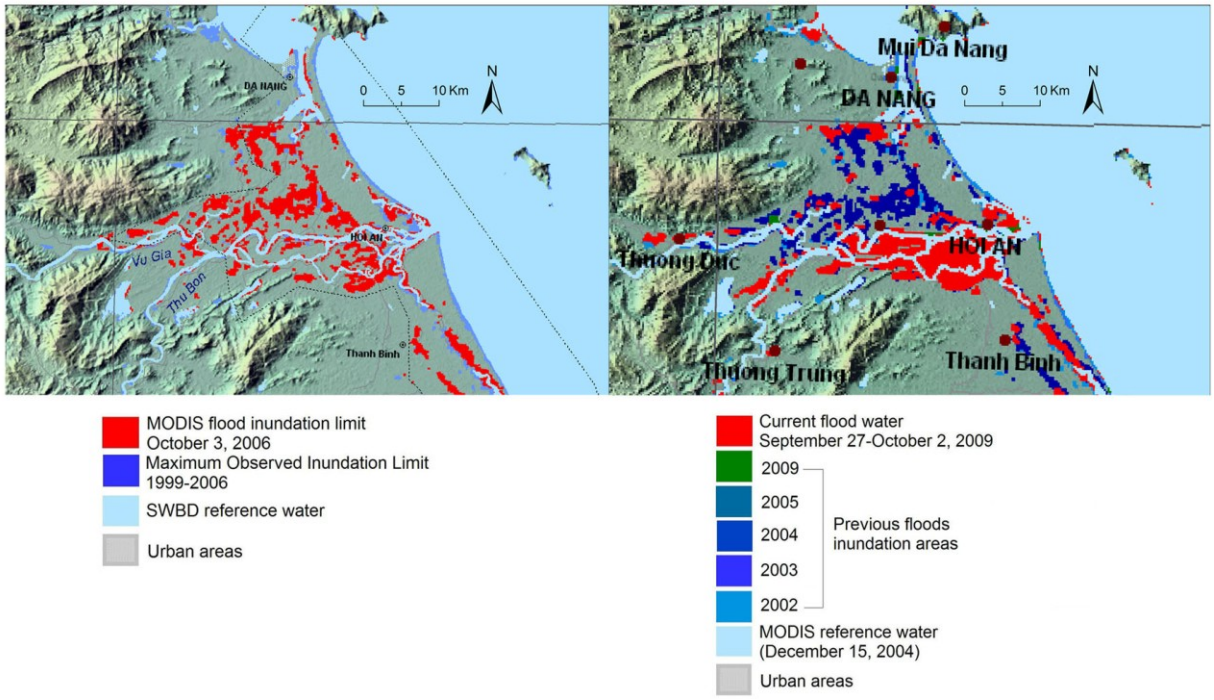

Fig. 16. MODIS rapid response flood inundation maps in the Danang area (a) on October 3, 2006 associated with Typhoon Xangsane and (b) from September 27 to October 3, 2009 associated with Typhoon Ketsana. Source: Dartmouth Flood Observatory (DFO).

The moderate hazard areas are distributed mainly at elevations higher than 6 m near the outlet for flood water from the upper parts of the two rivers. The inundation status of this area is not continuous in either of the MODIS flood inundation maps, but it is characterized by a high flood level (2.5-4.5 m) and drains well; thus, this region is designated as a flash flood area.

Flood basins and deltaic lowlands (back marshes) are subject to the deepest levels of inundation. Natural levees are designated as shallow flooding sites. Natural levees are associated with good drainage capacity, although the speeds of flood currents are likely to be high. The deltaic lowland is low and flat, but the inundation depth is not generally as deep as it is farther west in the flood basin because the floodwater can escape into the sea more easily. A comparison of the Hoi An flood height records with the landform map and the flood hazard map revealed a good fit between the flood conditions and the landform classification based on SRTM and LANDSAT data in this study.

2.5.4 Verification of results and field investigation

Although the SRTM DEM used in this study has a spatial resolution of 90 m, the digitizing process was conducted using LANDSAT images enhanced with the 15 m panchromatic band and the SRTM DEM as the reference DEM. Then, the landform map was verified and corrected using field observations, aerial photo interpretation, and topographic maps. Approximately 200 aerial photos taken in 1988 (scale 1:25,000, by Geology Union 6) covering almost the entire Thu Bon-Vu Gia plain were utilized to verify the landform classification map generated based on the LANDSAT ETM and SRTM DEM. The average elevations and flood hazard map were verified using topographic maps and field investigations.

The average elevation values were verified against the referenced elevation points from topographic maps in the plain area. All of the points selected for comparison with topographic maps to remove the overestimation error in lowland areas were located at bare, sparse or low vegetation sites (as discussed in Section 2.3.1). The average values were examined using elevation points with similar surface conditions on the topographic maps within each area of average values. The RMSEs associated with those average elevations were less than ± 0.5 m. The noise due to trees and buildings in the SRTM DEM in this area was not removed. However, such noise did not cause considerable interference with interpretation, calculation, and classification in this study.

The field investigation employed here consisted of observing landforms on the plain and measuring flood heights. The investigation revealed good results of the classification methods used in this study with 90 % of classified objects corresponding to those observed in the field. The classified features of mountains and hills, high and middle terraces, valley plains, flood basins, former river channels, deltaic lowland, sand dunes, inter-dune marsh, and water were clearly coincident with those that actually existed. Natural levees and lower terraces were confused with each other in some cases due to their similar elevations. Inaccurate objects were then corrected by reference to topographic maps and aerial photographs. The flood height and conditions corresponding to each landform unit were recorded for comparison. The field survey confirmed the correspondence and good fit between the observed landform characteristics and flood conditions.

2.6 Conclusions

The results of this study indicated that 43.34% of the Thu Bon plain is associated with a very high or high flood hazard in lowland areas (Hoi An city, Vinh Dien, Duy

Xuyen, Hoa Xuan), as well as a flashflood hazard in higher areas (Ai Nghia town, Dai Thang, Dai Cuong, Dai Phong).

The validated results display a good fit and correspondence with the landform classifications and flood hazard zonation, as well as the survey data. The methodology employed here for mapping landforms and flood hazard zones using satellite data (SRTM and LANDSAT) as primary material has demonstrated the usefulness of these data in places where topographic and land cover data are insufficient. SRTM DEMs provide valuable, consistent topographic data, and LANDSAT images provide land cover information. This geomorphological method of mapping flood hazards is useful when hydrological and meteorological data, or other information needed to develop a flood model, are limited and remote sensing images taken during flood events are not available. The small-scale landform classification maps produced using the open-source GRASS GIS provided significant 3D GIS cartographic support and functions that could be used to maximize and highlight terrain relief, as well as to visualize landforms in a sophisticated manner.

CHAPTER 3 – Rule-based landform classification by combining multi-spectral/temporal satellite data, and the SRTM DEM

3.1 Introduction

This chapter describes a rule-based landform classification in small scale for flood assessment. The rule-based method integrates land cover characteristics from multi-spectral/temporal remotely sensed data (Landsat and ASTER), local land-surface parameters from the SRTM DEM, and relative position analysis to classify landforms in a flat alluvial plain. The study area in this Chapter is the lower reach of the Vu Gia–Thu Bon river plain in central Vietnam as described in Chapter 2. This study showed the effectiveness of integrating land cover characteristics from multi-spectral/temporal remotely sensed data, local land-surface parameters from the SRTM DEM, and relative position analysis to classify landforms in a flat, alluvial plain. This interactive utility proved the significance of these factors in the landform classification of alluvial plains (Ho et al., 2012). The landform classification map by this method was compared to the manual map by visual interpretation produced by Ho and Umitsu (2011) (in Chapter 2).

3.2 Methodology

3.2.1 Data used and preprocessing

Table 2. Characteristics of the data used.

Data	Date	Resolution (m)	Season
Landsat MSS	June 3, 1973	80	dry
TM	August 24, 1990	30	dry
ETM+	March 23, 2001	30	dry
ETM+	March 16, 2007	30	dry
ETM+	December 21, 2007	30	rainy
ASTER VNIR	January 31, 2003	15	dry
SRTM	February 2000	90	

The data used are shown in Table 2. Only one image in the rainy season (December 21, 2007) was selected. Due to the fact that cloud coverage normally occurs in the rainy season, this rainy-season image showing clear moist surfaces without the cloud coverage is very valuable for classifying landforms in relation to flood inundation in this area. The rest images are in the dry season. The time-series images of the years 1973, 1990, 2001, and 2007 were chosen in comparable periods of time (dry season) to understand dynamic changes in this fluvial system governed by flooding from the past to present. The ASTER image with the higher resolution was used for obtaining land cover characteristics.

The SRTM DEM used in this study is WRS (World Reference System) tile, 3 arc-second (90-m) resolution, and filled-finished B set in path/row size (path 124–row 049) with GeoTIFF file format. The SRTM is known as the first ever high-resolution near-

global digital elevation data and providing a consistent-quality to give unprecedented opportunities for regional and global applications. SRTM DEM has proved huge applications on geosciences, especially geomorphology and hydrology (Zandbergen, 2008).

Before using SRTM data, pre-processing operations are required. The height overestimation in the SRTM DEM was eliminated over the entire plain by comparing with topographic maps in bare and/or sparse vegetated areas to determine the root mean square error of elevations (Ho and Umitsu, 2011). Then, to remove bias caused by trees and houses from the SRTM elevations after the elimination of height overestimation, the estimated average height of the coverage by trees and houses was subtracted from the elevations within the areas of vegetation and urban; the elevations of the other parts were remained unchanged. The bias by trees and houses was estimated by comparing the SRTM DEM with the 1:25,000 topographic maps of this area via the formula reported by Reuter et al. (2008) as below.

$$\delta_i = z_i^{TOPO} - z_i^{SRTM} \qquad (2)$$

3.2.2 Specification and computation of the inputs

According to Speight (1974), landforms are determined primarily based on elevation, relief, shape, size, orientation, contextual position, and moisture regimes. Therefore, the following inputs were used in this study:

- Classification of moist conditions by using the Modified Normalized Difference Water Index (MNDWI) and land cover (LC) characteristics derived from Landsat and ASTER data;

- Local relief of object edges (LRoE), average elevation (AVE), and channel features calculated from the SRTM DEM;
- Relative position indices including distances from the centroids of non-water objects to the river, the former river channel, and the dry riverbed (DIST) and the ratio of the border of each object with the river, the former river channel, and the dry riverbed to the entire border of non-water objects (RBR).

3.2.2.1 Classification of moist conditions using the MNDWI

Common methods to separate non-water and water features in a satellite image include the use of the slicing density of the near infrared (NIR) band to determine the threshold of water, combinations of relevant bands to highlight target features by maximizing or minimizing spectral characteristics, band ratios, and the Normalized Difference Water Index (NDWI) (e.g., Wang et al., 2002; Wang, 2004, Jain et al., 2005; Zheng et al., 2008). In particular, the NDWI approach by McFeeters (1996) takes advantage of the reflectance difference between water and non-water (land and terrestrial vegetated surface) of the green band and the NIR band in the equation (A-B)/(A+B), which is similar to the Normalized Difference Vegetation Index (NDVI) approach of creating a contrast of digital values and facilitating their extraction. However, the use of the $NDWI_{McFeeters}$ is affected by confusion between water and urban areas, which have similarly positive NDWI values. The MNDWI (Modified NDWI) by Xu (2006) solved this problem by using the combination of the green band and the middle infrared (MIR) band instead of the NIR band. Furthermore, the MNDWI can significantly help to isolate water and moist areas from non-water features. Such non-water features comprise not only urban areas but also sandy and vegetated surfaces because the MNDWI values of the water group are positive, whereas those of the non-

water group are negative. This finding suggests an effective method to isolate flooded areas or water-saturated areas with a high potential of being inundated in the rainy season images.

$$\text{MNDWI} = \frac{\text{Green}-\text{MIR}}{\text{Green}+\text{MIR}} \qquad (3)$$

With Landsat ETM+ data, the green band corresponds to band 2, and the MIR band corresponds to band 5. The MNDWI in this study was calculated from the Landsat ETM+ image from December 2007 (rainy season) to separate non-water areas from water and moist soil areas by determining thresholds. Ho et al. (2010) demonstrated the effectiveness of the MNDWI for separating moist surface conditions by use of thresholds as follows: $-1 \leq \text{MNDWI}_{\text{non-water}} < 0 \leq \text{MNDWI}_{\text{moist soil}} < \text{threshold} \leq \text{MNDWI}_{\text{water}} \leq 1$ (Fig. 17).

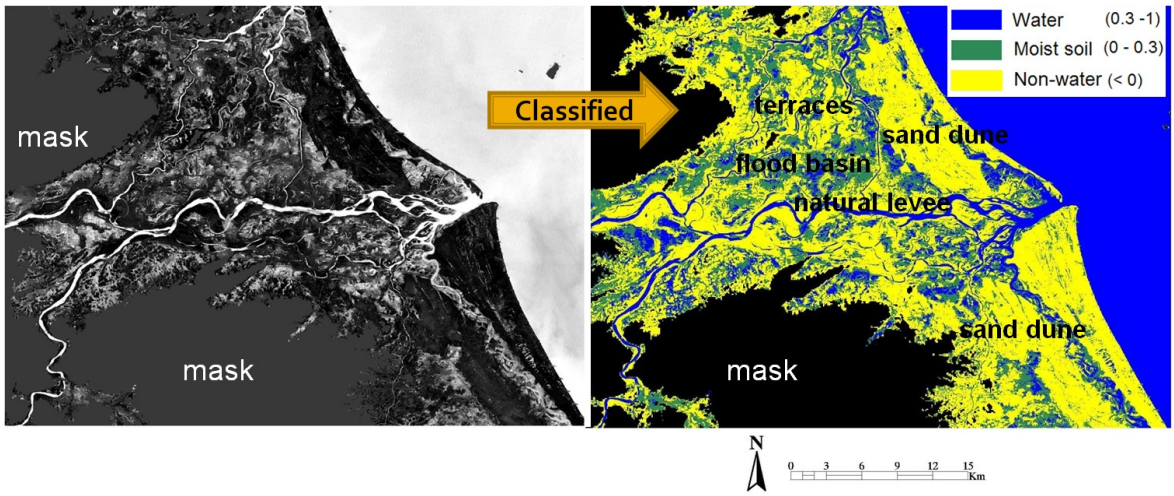

Fig. 17. The original MNDWI image of the Landsat ETM+ from December 21, 2007, after mountains and hills were masked (left part). The MNDWI image (right part) was classified into three categories: water (MNDWI 0.3–1), moist soil (MNDWI 0–0.3), and non-water (MNDWI ≤ 0).

In the case of the Landsat images from August 1990, March 2001, and March 2007 (dry season), the MNDWI thresholds were determined to isolate water from non-water areas for extracting water bodies in each of those years. With the Landsat MSS image from June 1973, the NIR band (band 6) was sliced to determine the threshold to separate river and lake areas in that year.

Because the target area is a low-lying alluvial plain, the thresholds of elevation (greater than 30 m), local relief (greater than 30 m), and slope (greater than 10%) (which are modified definitions of Speight, 1990) were applied to mask the high and upland areas composed of mountains, hills, plateaus, and upland basins (Fig. 17).

3.2.2.2 Land cover classification and channel network

The ISODATA unsupervised classification of the ASTER image was undertaken with 50 clusters. Then, a reclassification process was performed to generate six land cover categories: forest, agricultural land, sandy soil, bare soil, wet land, and urban. Although the more clusters the image is divided into, the better the classified result may be, 50 clusters is appropriate to classify into the six land cover types in this study.

3.2.2.3 Extraction of channel features (CFs)

Channels were also detected using the GRASS GIS function called r.param.scale, which calculates and classifies the terrain features: planar, pit, channel, pass, ridge, and peak (Wood, 1996). The channel extraction performed by this function helped to identify low depressions. These channel features commonly represent channel morphologies such as former river channel, dry riverbed, and valley plain areas. In particular, when such low depressions cannot be isolated by the MNDWI classification,

land cover classification, or the composite Landsat image, channel features help to separate non-water polygons from areas of extremely low elevation (low depressions) (Fig. 18).

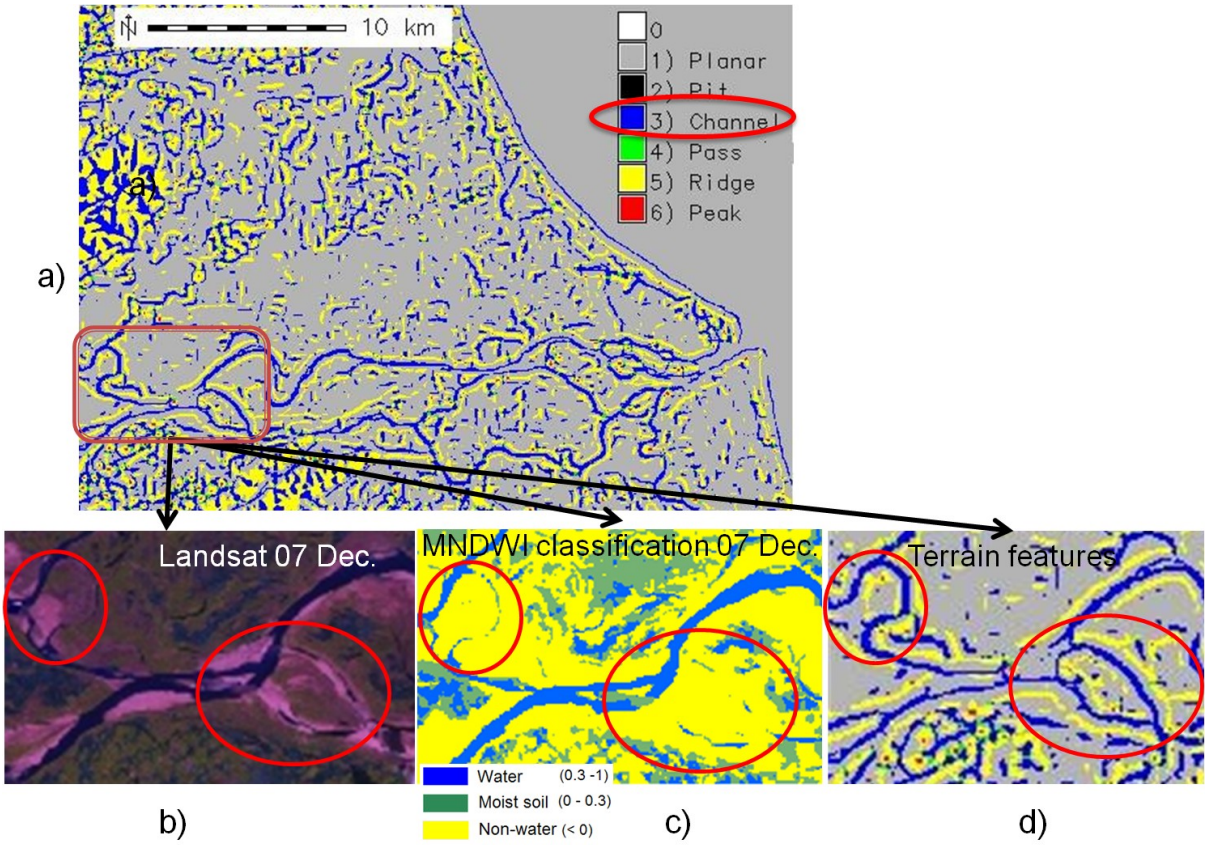

Fig. 18. The r.param.scale function can help to extract channel features (low depressions) (a, d) that are difficult to be detected in the composite Landsat image (b), and they appear as non-water features in the MNDWI classification (c).

3.2.2.4 Local relief

Relief is defined as a difference in elevation between the high and low points of a land surface. Local relief is the relief within a certain area (Coops et al., 1998).

$$\text{Local relief} = \max_{i \epsilon C} z_i - \min_{i \epsilon C} z_i \quad (4)$$

- max z_i: the highest elevation value within a moving window C of defined sides (3 x 3, 5 x 5 … size) with a center i,
- min z_i: the lowest elevation within this moving window,

The local relief values were calculated by a 3 x 3 square moving window (Fig. 19a). Local relief is a useful parameter for identifying small-scale landforms because it indicates differences in relative elevations. Next, average local relief values were calculated within the 120-meter internal buffers of the edges of the non-water polygons (Fig. 19b).

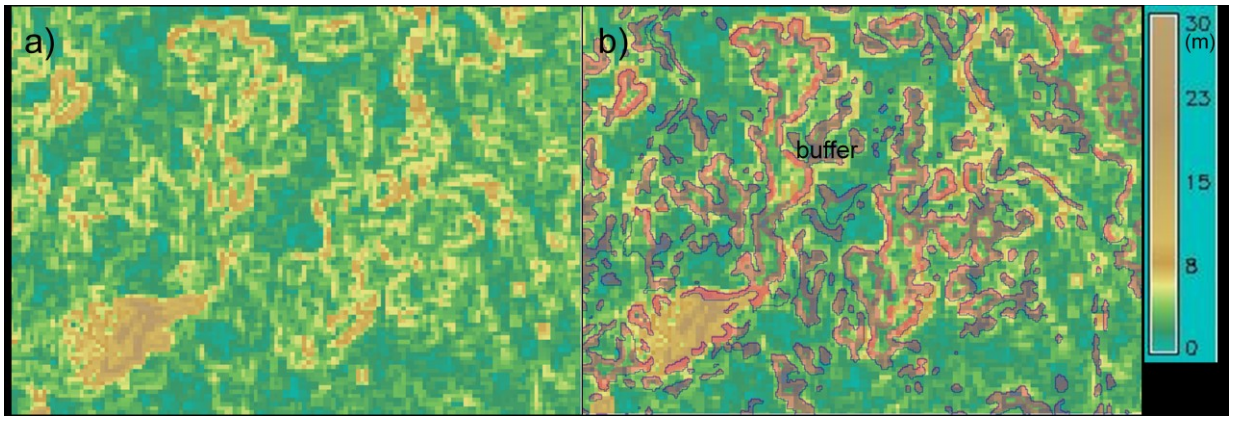

Fig. 19. Notably higher local relief values (a) within the internal buffers (the pink areas in the image b) of the edges of non-water objects indicate the scarps of terraces.

3.2.2.5 Average elevation

Average elevation is defined as an average value calculated for each target polygon.

$$\bar{z} = \frac{1}{n}(z_1 + z_2 + \ldots + z_n) = \frac{1}{n}\sum_{i=1}^{n} z_i \quad (5)$$

$\bar{z}$: the average elevation value,

n: the total number of pixels in the target polygon,

z_1, z_2 …, z_n: all of the elevation values of the target polygon.

3.2.2.6 Relative position indices

Relative position indices indicate the contextual position of each landform. The relative position relies on the nature of landforms, for example, natural levees are formed along rivers and/or former river channels, whereas sand dunes are situated parallel to the coastline. The relative position indices were used to determine landform objects that have similar characteristics of the above indicators. Relative position indices are represented by the distance to the river, former river channel or dry river bed (DIST) and the ratio of the border of a non-water object with the river to the entire border of that object (RBR) (Fig. 20). The RBR indicates how much an object is covered by river, former river channel, and dry river bed areas.

$$RBR = \frac{length\ of\ border\ with\ river}{length\ of\ the\ entire\ border} \quad (6)$$

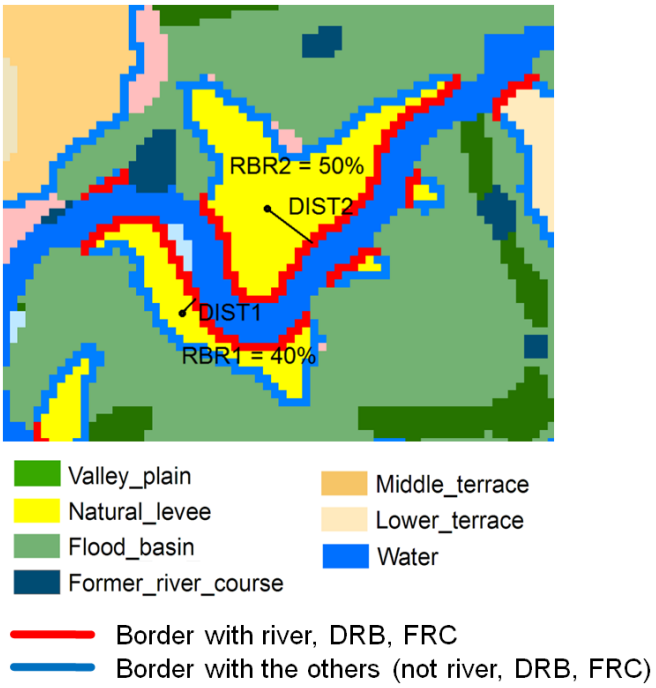

Fig. 20. Distance to river indicates the minimum distance from the centroid of a non-water object to the nearest river, former river channel, or dry river bed objects. The percentage of the total border that borders a river, former river, or dry river (RBR) indicates the water-bordering fraction of a non-water object by dividing the water-bordering length of the border by the entire border length of the object. The DIST and RBR were used to distinguish natural levees from the other non-water features (terraces, sand dunes). See the detailed rules of the classification in the section 3.2.3 below.

3.2.3 The rule-based landform classification

The general process of the rule-based landform classification was based on a hierarchical rule by which pixels and objects are separated (Fig. 21).

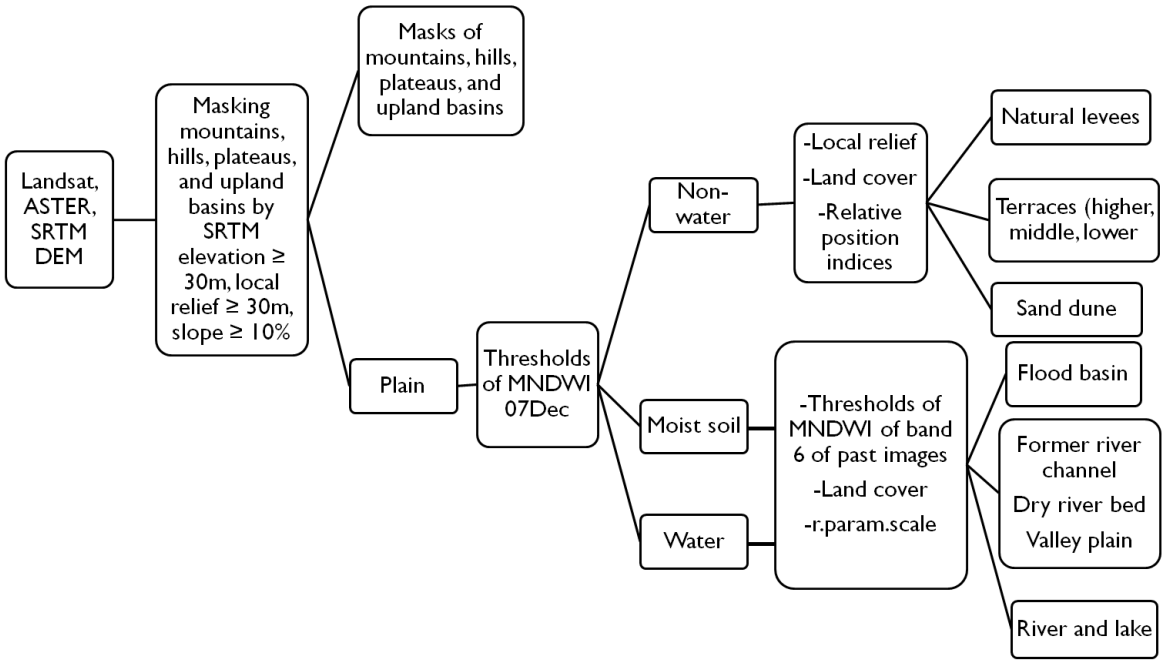

Fig. 21. The flow chart for the rule-based classification of small-scale landforms.

The landform categories were classified into three groups: water, moist soil, and non-water areas. The water group consists of permanent water including rivers, lakes, and sea and temporal water stagnating in low areas in the rainy season. The moist soil group consists of low-lying landforms such as flood basins (also back swamp, which is usually used for paddy fields), valley plains, former river channels, dry riverbeds, and inter-dune marsh. Such low-lying surfaces usually catch overbanking flow, particularly in rainy seasons, thus, these landforms are vulnerable to flooding. In addition, their primary sediment material is clay, which can absorb and maintain water and/or moisture. Therefore, these surfaces commonly appear to be wetter than neighboring higher areas, especially when the paddy fields are not in the growing period and witnessed as bare-moist soil. In contrast, the non-water group comprises high-lying areas with frequently dry conditions consisting of natural levees, terraces, and sand dunes that do not become submerged in flood time. Hence, the non-water landforms are

invulnerable to flooding (terraces and sand dunes) or, if they are submerged, are well drained (natural levees). Also, their composition consists of silt and sand as the main sediment materials, which means that they are unlikely to hold water. Such characteristics of these groups are more obvious in the rainy season, when a large amount of rainfall is concentrated on the plain (Ho and Umitsu, 2011). Thus, the wetness of the landform surface is a critical indicator for distinguishing these groups of landforms in an alluvial plain.

In short, small-scale landforms (LF) are classified according to the following rules:

- Permanent water (river and lake): if water is indicated in all of the satellite data (MSS 1973 June, TM 1990 August, ETM+ 2001 March, ETM+ 2007 March, and ETM+ 2007 December);
- Flood basin (FB): if (moist soil in MNDWI of ETM+ 2007 December) or (paddy field in the land cover images of ASTER and ETM+ 2007 March);
- Natural levee (NL): if (non-water in MNDWI of ETM+ 2007 December) and (RBR $\geq$ threshold or DIST $\leq$ threshold or LRoE ≤ 2 or AVE ≤ 3);
- Former river channel (FRC): if (water in MSS 1973 June or TM 1990 August or ETM+ 2001 March) and (non-water in ETM+ 2007 March or ETM+ 2007 December);
- Dry river bed (DRB): if (LF = channel) and (LC = sand) and (adjacent to river);
- Valley plain (VP): if (LF = channel) and (LF $\neq$ former river channel and LF $\neq$ dry riverbed);
- Sand dune (SD): if (non-water in ETM+ 2007 December) and (LC dominated by sand) and ($2 <$ LRoE ≤ 3 and DIST > threshold); and

- Terrace (TR): if (non-water in ETM+ 2007 December) and (RBR < threshold and DIST > threshold);
    - else if 3 < LRoE ≤ 4: lower terrace (LTR)
    - else if 4 < LRoE ≤ 5: middle terrace (MTR)
    - else if LRoE > 5: higher terrace (HTR)

The thresholds of LRoE, RBR, DIST, and AVE were set based on the characteristics of each landform feature in this area. These indices can be applied for other areas but need to adjust the thresholds depending on the features of landforms in each area.

The LRoE threshold was determined depending on the relative height of each terrace type (lower, middle, and higher) that is measured in field and from the topographic map in this study area. The local relief indicates the relative elevation. High values of the local relief indicate local scarp of an elevated object whereas its low values indicate the relatively flat surface. Thus, it is used to identify elevation-homogeneous elevated surface such as terraces.

The RBR and DIST thresholds were set among non-water and elevated landform features (terraces, sand dunes, and natural levees) after being classified by MNDWI classification and LRoE thresholding.

The RBR indicates the coverage degree of a river with a landform object; particularly this index is useful to recognize natural levees. In common, natural levees situate along two sides of a river, as a result empirically about more than two-third portion of their border embedded by a river. Thus, the thresholds of RBR are more than 30%.

The DIST index is also useful to identify natural levees that have elongate shape but have uncontinuous borders with a river. Meanwhile the RBR index is more appropriate

to distinguish natural levees that have shorter and larger shape and have continuous border with a river. The threshold of DIST is less than approximately 5 pixels equivalent to 150 m with 30 m grid size in this area.

The AVE threshold was applied for natural levees situated near deltaic low land near the estuary of the Thu Bon river.

Although the rule-based small-scale landform classification in this study is primarily object-based, the salt and pepper effect results from the pixel-based steps of MNDWI classification, river extraction, land cover classification. Therefore, the rule-based landform classification result was smoothed using the majority method by filtering the most frequently occurring value within the 5 x 5 moving window. Despite the availability of advanced techniques to reduce the "salt and pepper" effect such as Markov Random Field and image segmentation, we did not concentrate on this matter because the main objective of this study is proposing a framework of the rule-based landform classification. Moreover, the majority filter provided acceptable and reasonable accuracy in the previous studies and this study as well.

3.3 Results and discussion

3.3.1 Evaluation of the rule-based landform classification method

The rule-based landform classification method was evaluated by comparing the statistics of the MNDWI classification with the landform categories of the manual LCM and local relief.

The comparisons in Table 3 demonstrate that the MNDWI works well for separating the representative groups and identifying polygon boundaries in the early

stages of applying the method because of its good correlation with the manual LCM categories and local relief ranges.

First, the non-water, moist soil, and water categories of MNDWI classification were compared visually with the manual LCM. Figure 22 indicates that the moist soil areas had a high coincidence with the flood basin and valley plain areas of the manual LCM, which are commonly submerged during times of flooding. Figure 23 shows that the non-water areas were well matched with the levees, sand dunes, and terraces.

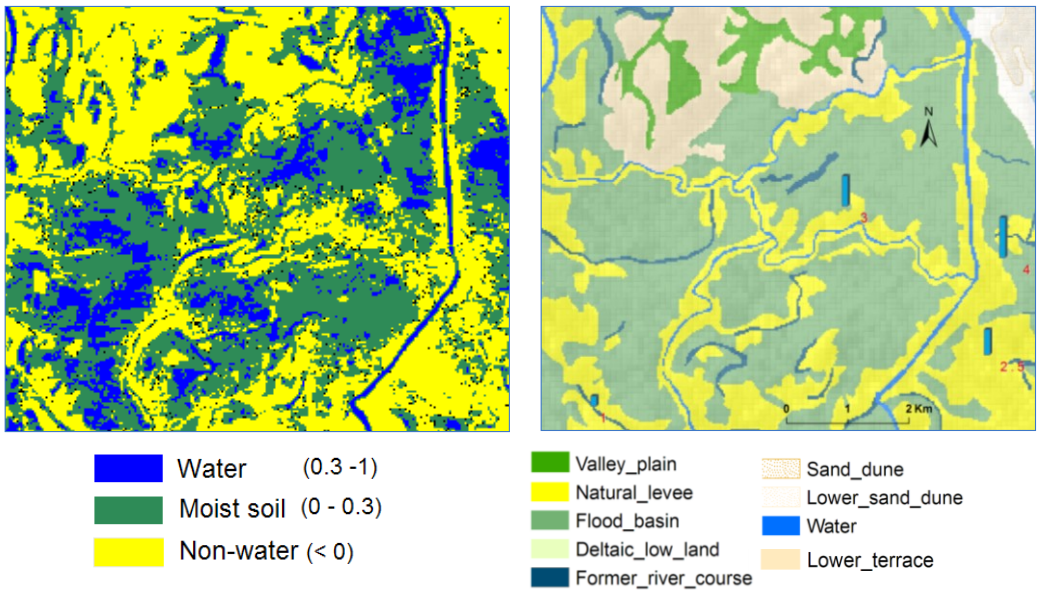

Fig. 22. The left-hand side shows the MNDWI after categorization into three classes, and the right-hand side is the manual landform classification map. With the exception of permanent water such as rivers and channels, only temporal water is seen in the moist soil areas. The blue (temporal water) and green (moist soil) parts of the MNDWI image coincide well with the flood basin in the landform classification map. The yellow areas (non-water) in the left-hand image share a similar pattern with the natural levees and terraces in the right-hand image.

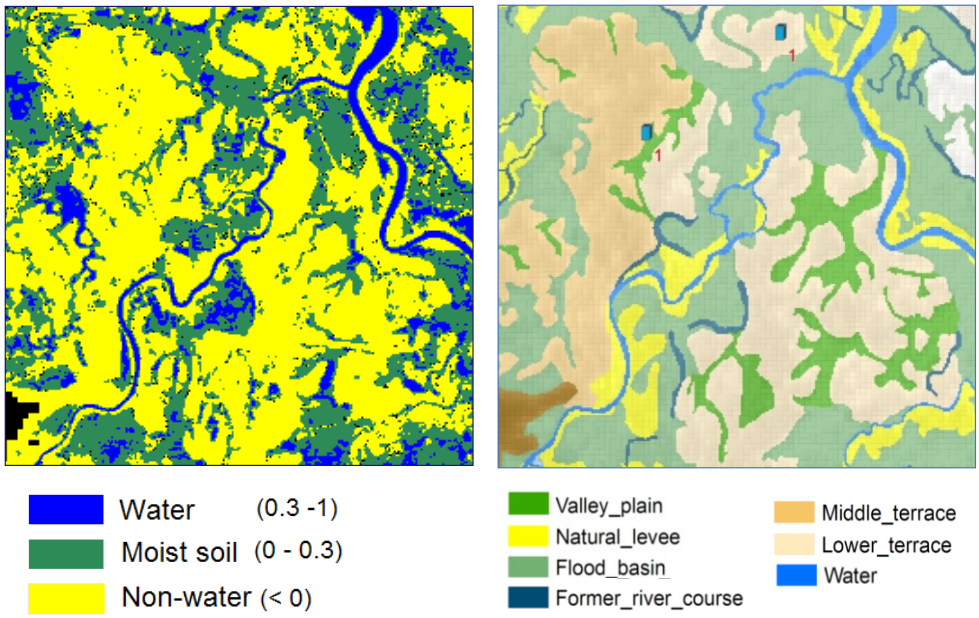

Fig. 23. Good agreement is shown between the non-water (yellow) parts of the MNDWI image (after classification) (left) and the terrace areas of the manual landform classification map (right).

For quantitative evaluation, the categories of non-water, moist soil, and water determined by MNDWI classification in the December 2007 Landsat image were compared with the three landform groups in the manual landform classification map and two ranges of local relief (Table 3).

Table 3. Statistics of the non-water, moist soil, and water classes of MNDWI classification compared with landform categories and local relief

		MNDWI classification		
		Non-water (%)	Moist soil (%)	Water (%)
Manual LCM	Flood basin, valley plain, former river channel, and dry riverbed	29.89	79.74	19.55
	Natural levee, terrace, and sand dune	68.49	17.03	8.34
	River and lake	1.62	3.23	72.11
Local relief	≤ 2 m	65.38	80.38	
	> 2 m	34.62	19.62	

Table 3 reveals good agreement between the MNDWI classification results and the landform groups on the manual landform classification map. The percentage of agreement between the moist soil class and the landform groups of FB, VL, FRC, and DRB on the manual map is 79.74%, whereas the agreement between the non-water class and the landform groups of NL, TR, and SD on the manual map is 68.49%. The former group is located at low elevations and has a high inundation potential, whereas the latter group is at high elevations and has a low inundation potential in the rainy season.

On the one hand, a comparison of moist soil and non-water areas and local relief shows that the moist soil class covers only 19.62% of local relief values > 2 m, whereas moist soil covers 80.38% of local relief values ≤ 2 m. The non-water class covers

34.62% of local relief values > 2 m and 65.38% of local relief values ≤ 2 m. From these numbers, it can be inferred that most of the high local relief values are distributed within the non-water class and that such high local relief values exist at the boundaries of polygons. On the other hand, a large amount of local relief values ≤ 2 m belongs to the non-water class because the inner areas of the non-water features (terraces, natural levees, and sand dunes), with the exception of the boundaries of the polygons, are commonly flat, and hence the local relief of such inner areas is usually low. In general, although the low local relief values (≤ 2 m) dominate in either the non-water or the moist soil class because of the flatness and low relief of most of the landform surfaces in the alluvial plain, high local relief values (> 2 m) are more dominant in the non-water class (distributing at the edges of the non-water features) than in the moist soil class.

3.3.2 The rule-based landform classification map

The scale of the rule-based landform classification map is designated based on the pixel size of Landsat TM/ETM+ (30 m). According to Hengl (2006), the cell size is equal to 0.5 mm on a paper map. In other words, the 30-m resolution of the grid of the rule-based map corresponds to a 1:60,000-scale map.

The "mountain and hill" category did not exist in the rule-based landform classification map because it was masked, as described previously. The same mask was applied to the manual map to make it consistent with the rule-based map. However, several areas of mountain and hill remained on the manual map.

3.3.3 Comparing the rule-based landform classification maps with the manual one

Small-scale landform features of the rule-based LCM were compared with those of the manual LCM that was validated by Ho and Umitsu (2011). These two maps were

compared by considering only the landform categories existing on both maps. The rule-based LCM shows a high correlation with the manual LCM by visual comparison (Fig. 24).

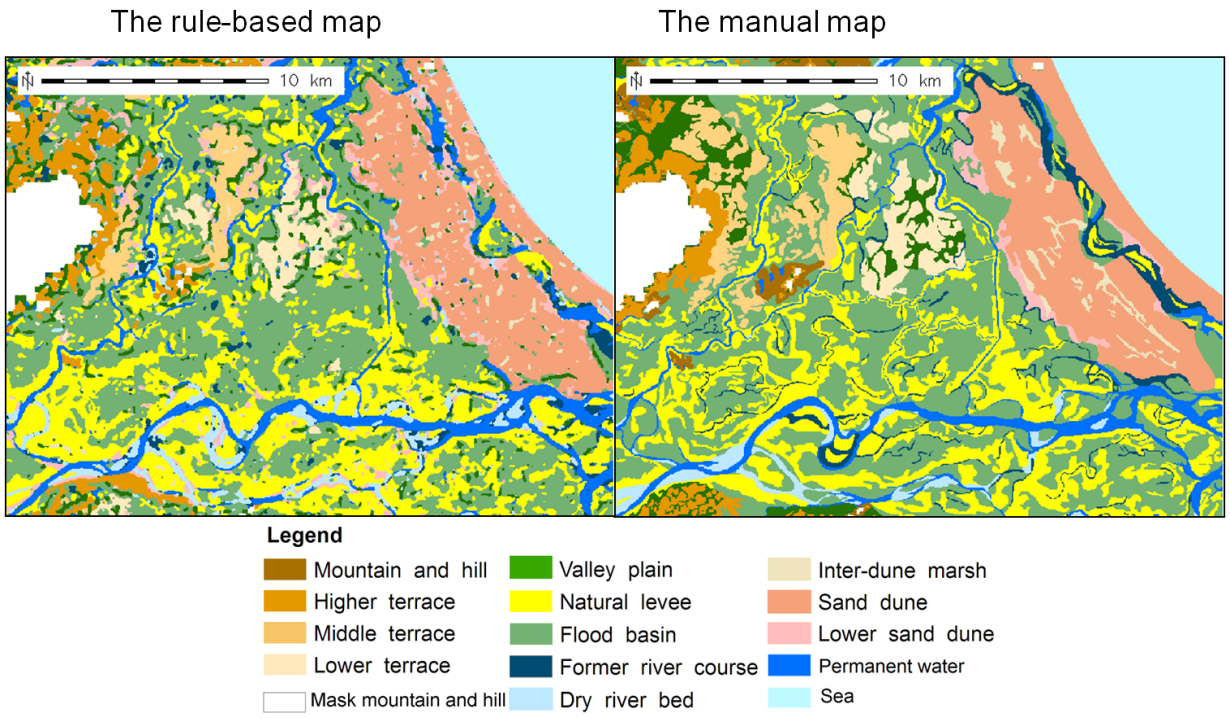

Fig. 24. The rule-based small-scale landform classification map (left) compared to the manual map (right).

The overall similarity of the rule-based map compared to the manual one is 58.1% done by the overlay statistical method. This modest accuracy is resulted from (1) the subjectivity existing in the manual map that is overcome by the rule-based method and (2) the limitations and difficulties of the rule-based mapping method for identifying small objects.

The discussion focuses on the main landform categories that dominate this alluvial plain and contribute to explain the flood inundation conditions such as terraces, flood basin, natural levees, sand dunes (high accuracy), former river channel, dry river bed, and valley plain (lower accuracy). The high-accuracy group has significant similarities,

which demonstrates the efficiency of the rule-based method for the landform classification. The lower-accuracy group accounts for the modesty of the overall similarity. In other words, it indicates the limitation and difficulties of the rule-based mapping method using medium resolution data. In addition, the lower-accuracy group also reveals the subjectivity of landform classification by the manual method. Although the manual landform classification map was validated with 90% accuracy by the field investigation combined with aerial photos and topographic maps (Ho and Umitsu, 2011), there are some features and/or objects that make confusing. Those can be identified evidently by the rule-based process. Because Ho and Umitsu (2011) investigated and verified randomly around the study area where the authors could access, and allocated most of the categories of the landform but did not cover all of objects. Therefore, for instance, the large areas of each level of terraces were investigated, but the other small parts of terraces were paid less attention. In other studies (Speight, 1974, 1990; Van Westen, 1993) and our opinion, the field investigation, interpretation of aerial photos, and topographic maps are the key processes of the manual method, but at the same time, are affected by human subjectivity. Furthermore, the boundary delineation of the landform objects by the manual method normally relies on the interpretation and experiences of the person creating the map (Klingseisen et al., 2008). Therefore, even the manual map was validated, its boundary delineation has a certain degree of subjectivity. These shortcomings can be overcome by the rule-based method.

3.3.3.1 Extraction of terraces

The similarity of terraces between the rule-based and manual LCMs is 37.9% for the higher terrace, 66.7% for the middle terrace, and 57.5% for the lower terraces.

Misclassification may occur among higher, middle, and lower terraces of the manual LCM, which can cause low accuracy for each terrace classification of the rule-based LCM. However, these misclassifications are likely caused by the subjective interpretation of various levels of terraces when creating the manual map. Figure 25 presents an example of the misclassification of a lower terrace. Another statistic by comparing the total area of the terraces of the rule-based LCM with that of the manual LCM reveals that the total similarity of the terraces is higher than 80%.

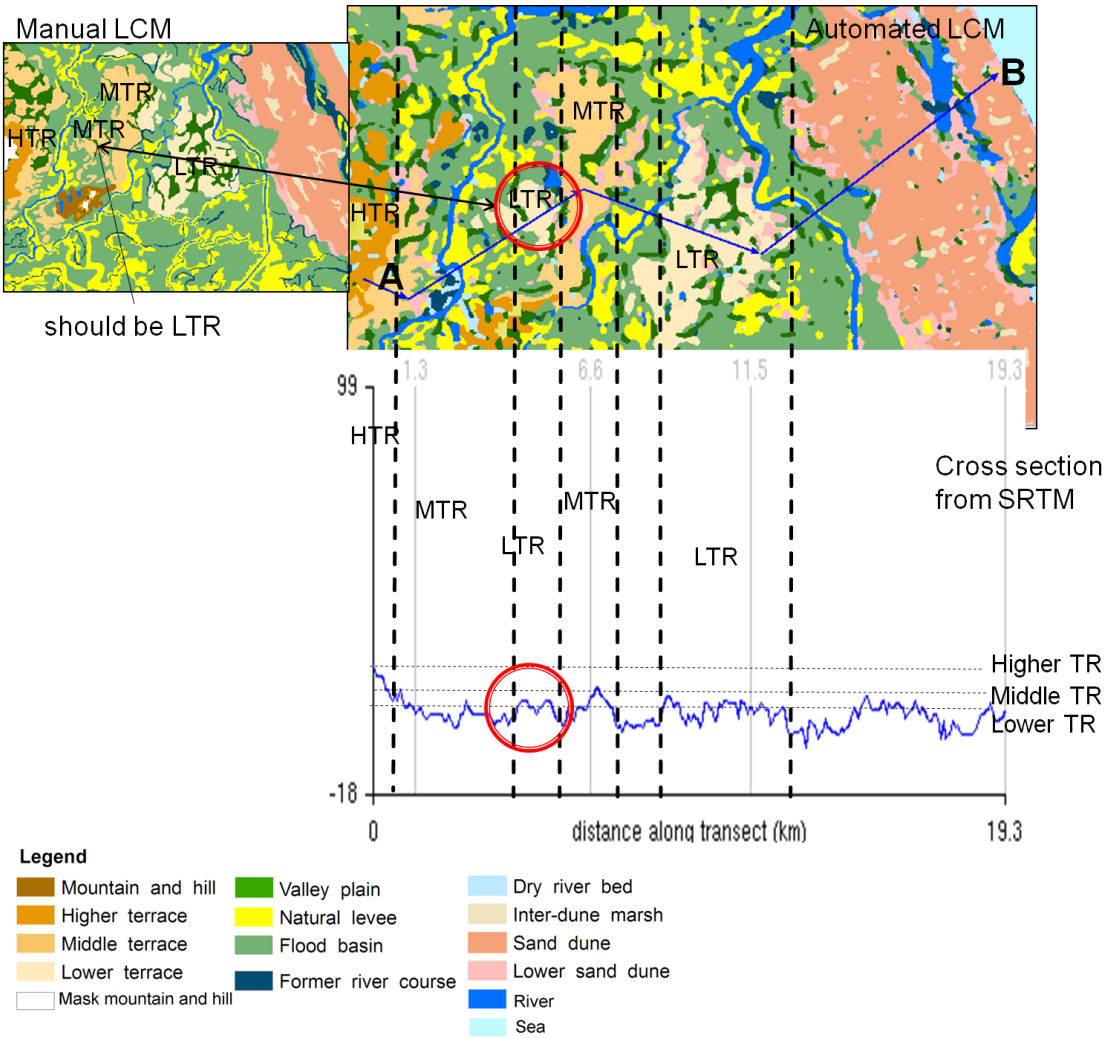

Fig. 25. The lower terrace (the upper red circle) classified on the rule-based LCM (right) appears as a middle terrace on the manual LCM (left). The cross section derived from the SRTM DEM affirms that the average level of this lower terrace (the lower red circle) is lower than that of the middle and higher terraces.

The classification of terrace levels is a challenge. In common, most of the landform categories are rather evident to distinguish because their characteristics are clear. Nevertheless, the cases between lower and middle terraces and between lower terraces and natural levees are special and more difficult to classify even by using aerial photo stereo-scoping although their separation is crucial for understanding flood conditions of a floodplain.

3.3.3.2 Extraction of flood basins and natural levees

The accuracy of the flood basin classification of the rule-based LCM is 67.4%, and the misclassification of the flood basin as the valley plain and the former river channel is 5.1% and 4.7%, respectively, on the manual LCM. However, the flood-affected degree of the valley plain and the former river channel is similar the flood basin. Therefore, this misclassification causes inconsiderable problems in the prediction of flood susceptibility

The rate of misclassification of the flood basin as the natural levee is 17.2%. Such natural levees are small and narrow. They appear as moist soil in the MNDWI classification, are usually submerged in times of flooding, and are not useful for human settlement (Fig. 26). Thus, this misclassification is also unremarkable for the goal of flood assessment.

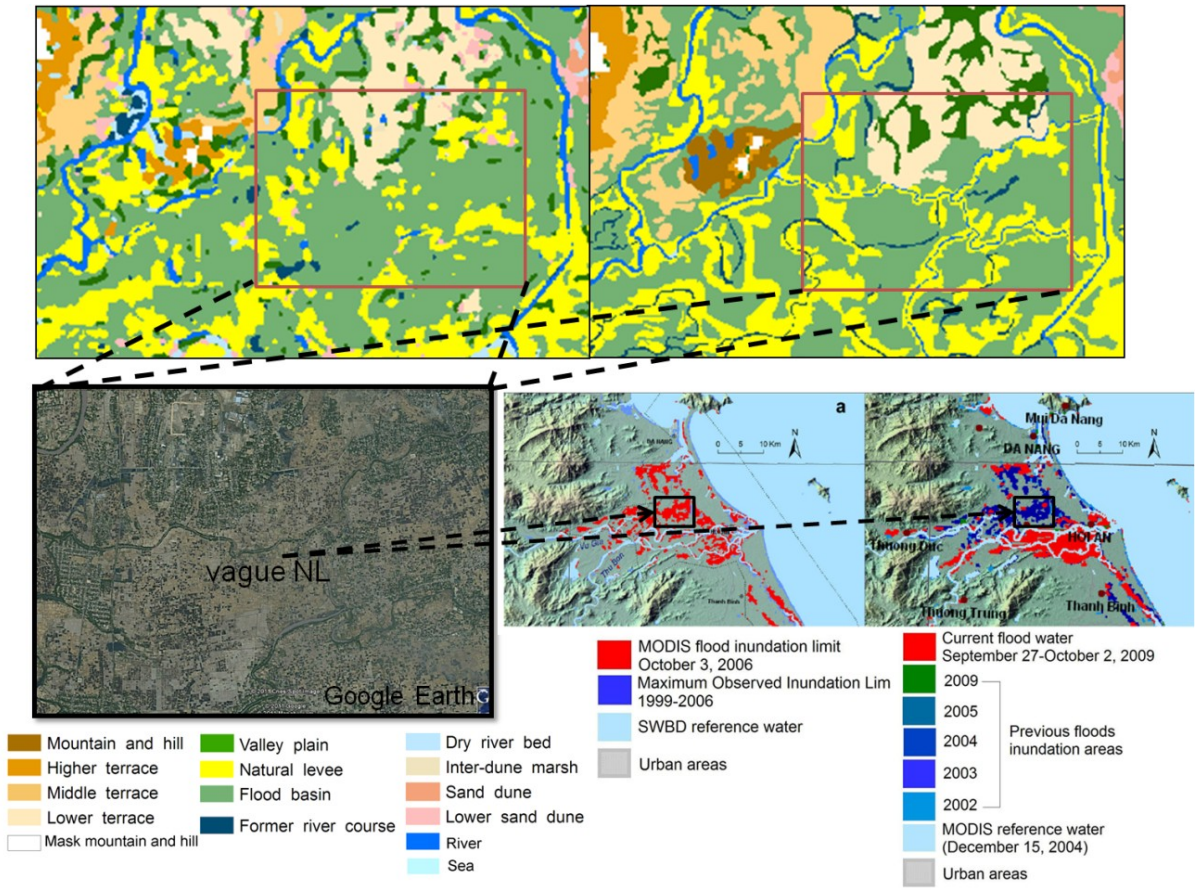

Fig. 26. The small and narrow natural levees that are shown on the manual LCM (upper right) were not detected in the semi-automated LCM (upper left). These natural levees are slightly visible on a 2008 Google Earth map. Moreover, they were inundated in 2006 (normal flood event) or 2009 (severe flood event).

3.3.3.3 Extraction of sand dunes

The comparison demonstrated that sand dunes on the rule-based map have 87.5% coincidence with those on the manual map. This high agreement is a result of the stability, large size, and clear boundaries of the sand dunes.

3.3.3.4 Extraction of river networks, former river channels, dry riverbeds, and valley plains

The river network determined by multi-temporal images was classified more precisely than those on the manual map based on a single-year image. The recent river network can be extracted from the present images or the newest image of a dataset. Dry river beds and former river channels have modest accuracies due to the limitation on the data used resolution. Those two landform categories commonly comprises small objects that are difficult to be extracted based on the SRTM DEM and Landsat data, but can be identified by visual interpretation. However, the larger objects of dry river beds and former river channels can be identified advantageously and subjectively by the past river network, which can be derived from the past images. Valley plains on the two maps were visually compared and showed good coincidence with the channel feature by the function r.param.scale in spite of less similarity with that of the manual map.

3.4 Conclusions

The rule-based landform classification method achieved by combining the SRTM DEM and multi-temporal satellite images is effective and promising for classifying small-scale landforms in alluvial plains. Furthermore, this rule-based method is objective, simple to edit, and saves much more time than the manual method. The remarkable advantage of this method is that it produces more objective classifications than a manual method because it quantifies the characteristics derived from satellite images and the SRTM DEM. Mountains and hills are defined (masked) by thresholds of elevation, local relief, and slope, and thus more reliable. Sand dunes are identified with high accuracy. Terraces are separated objectively by local relief and average

elevation. Flood basins are classified in close relationship to the moist condition, which makes the data convenient for predicting areas that might be affected by flooding. The use of multi-temporal satellite images helps to classify river network more precisely and to identify dry river beds and former river channel areas effectively. However, limitations on the spatial resolution of satellite data and the SRTM DEM create difficulty in identifying small-size landforms such as narrow rivers, former river channels, dry riverbeds, and narrow natural levees that can be identified well by visual interpretation. However, these limitations have only insignificant effects on the prediction of areas that are susceptible to flooding. Thus, this method is effective and suitable for flood hazard assessment. In particular, this method would be useful in developing countries because it enables the creation of landform classification maps that are consistent with manual LCMs by visual interpretation.

CHAPTER 4 – Delineation of small-scale landforms in relation to flood inundation in the western part of Red River delta, north Vietnam

4.1 Introduction

To generalize the rule-based method to apply for different alluvial floodplains and make it more convincing, this chapter describes adjustments to the rule-based landform classification method proposed by Ho et al. (2012) for a case study on the western plain of the Red River delta, northern Vietnam, for the evaluation of flood susceptibility. The overall landform classification was compared visually to the map generated manually, and landform boundary delineation was verified using flood extent derived from the Landsat ETM+ image of the 2001 flood based on the relationship between landforms and flood conditions.

4.2 Study area

The study area is the western Red River delta, northern Vietnam, including the capital city of Hanoi and surrounding areas (approximately 2595 km^2; Fig. 28). Hanoi is located at the confluence of the Red River and the Duong River, along the western bank of the Red River. The study area includes most of the fluvial-dominated plain adjacent to the wave-dominated plain in the southwest and the tidal-dominated plain in the northeastern part of the delta (Mathers et al., 1996; Mathers and Zalasiewicz, 1999; Tanabe et al., 2003; Funabiki et al., 2007 and 2012). The fluvial flux is strong compared to the other two systems (Tanabe et al., 2003). This fluvial-dominated system consists of meandering rivers and levee belts, floodplain, and fluvial terraces. Natural

levees, rising 2–5 m above the adjacent back swamp, are formed along the Red River, Day River, and Duong River and along abandoned river channels, with absolute elevation of approximately 5–10 m. Back marshes are formed at elevation 3–5 m between the natural levees, particularly between the Day River and the main tributary of the Red River (Funabiki et al., 2007 and 2012).

The water discharge varies seasonally due to a subtropical monsoon climate regime. The maximum discharge recorded at Hanoi station in July–August is about 23 000 m^3 /s and the minimum one during the dry season (January–May) is approximately 700 m^3 /s (Mathers et al., 1996; Mathers and Zalasiewicz, 1999).

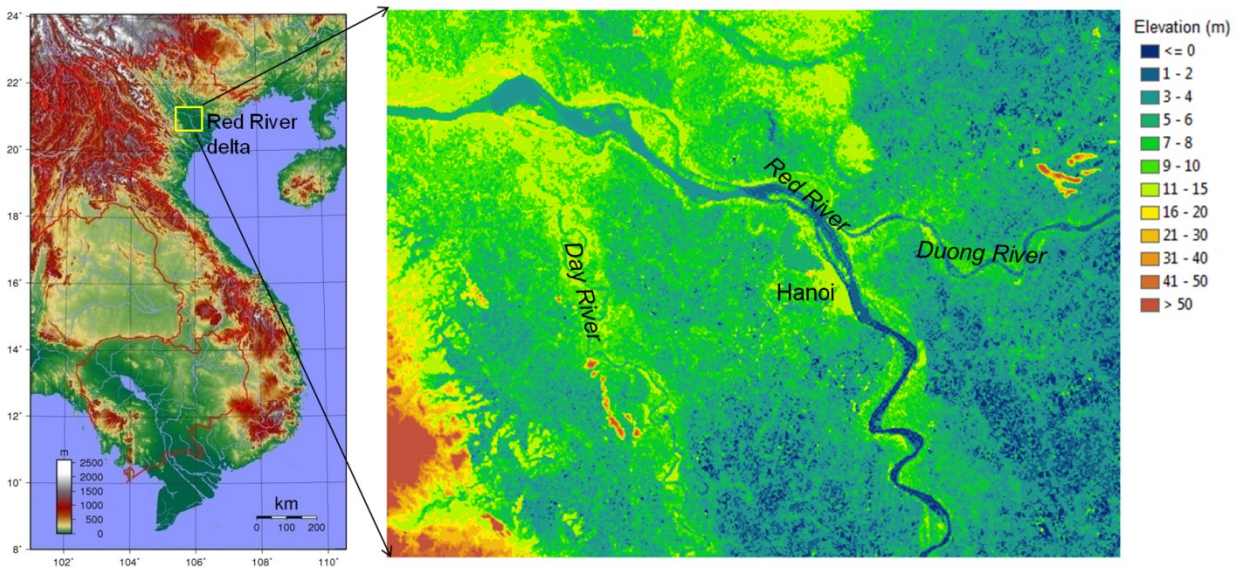

Fig. 27. Study area – the western part of the Red River delta, including Hanoi and the surrounding area.

Hanoi is one of the two largest economic centers in Vietnam, along with Ho Chi Minh City in the South. The central urban area of Hanoi has expanded in all directions, but primarily to the south, southwest, west, and, recently, to the east. Despite robust urbanization, much of this area is still maintained as croplands (back swamp), which

are an important source of food and other agricultural products for Hanoi (Kono and Doan, 1995; Mathers and Zalasiewicz, 1999). Urbanization in Hanoi has accelerated since the introduction of Doi Moi (Economic Renovation Policy) in the late 1980s (Ho and Shibayama, 2009). Increasing urban development over the back swamp causes flood susceptibility and diminishes flood drainage surface (Dang et al, 2011).

The average rainfall in this area is approximately 1400-2000 mm/year. In 2008, heavy rain in the Red River delta from October 30 to November 1 resulted in large-scale flooding in Hanoi. Rainfall in Hanoi during that time was up to 500 mm, which is the highest recorded rainfall in a single event since 1978 (Fig. 29) (Institute of Geography Vietnam, 2008).

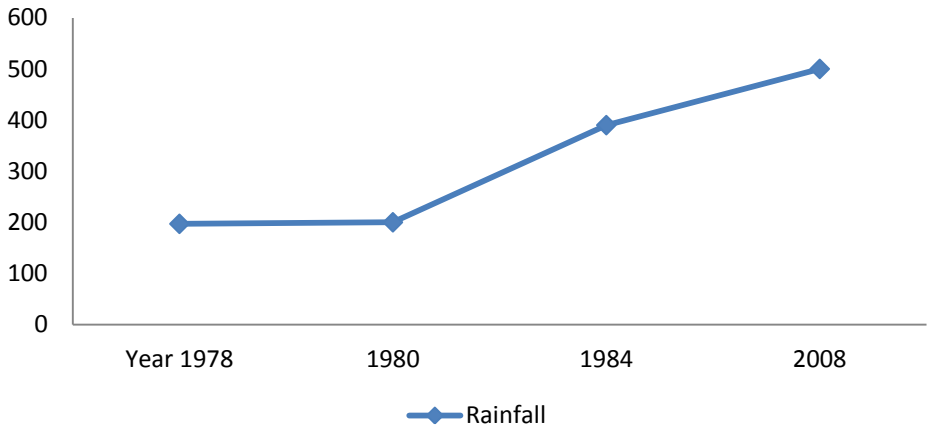

Fig. 28. The highest rainfall observed in a single rain event from 1978 to 2008 in Hanoi.

4.3 Materials and methods

4.3.1 Remotely sensed data for processing and validation

Table 4. Description of data used.

Data	Date	Resolution (m)	Description	Bands used	Used for
Landsat MSS	December 29, 1975	80	Cropland in non-growing season	2 and 5	Extracting the past river network
TM	December 27, 1993	30	Cropland in non-growing season	2 and 5	Extracting the past river network
ETM+	November 4, 2000	30	Cropland in non-growing season	1 – 7	Extracting the past river network Classifying land cover for enhancing the SRTM DEM
ETM+	July 18, 2001	30	• Captured during a heavy rain period that caused a historical flood event in late July, 2001 • Cloudy in central and northern Hanoi • Cropland in non-growing season		Validation
ETM+	November 8, 2007	30		1 – 7	Classifying land cover
ETM+	November 10, 2008	30	• Captured after the flood peak of the severe flood event in 2008 • Cropland in non-growing season	2 and 5	Extracting post-flood areas
SRTM DEM	February, 2000	90			Calculating local land-surface parameters

Five Landsat images from path 127 – row 45 were used for the rule-based procedure outlined below, and one was used for validation. Four images were acquired at a similar season of year (MSS 1975 December 29, TM 1993 December 27, ETM+ 2000 November 4, and ETM+ 2007 November 8) (Table 4) and used to extract river network and former river channels, using bands 2 and 5 for calculating the Modified Normalized Different Water Index (MNDWI). The November 4, 2000 image was used for land cover classification. The ETM+ post-flood image from November 10, 2008, captured approximately one week after the peak flood time, was used to identify recent wet, moist, and dry areas. The July 18, 2001 image was captured during heavy rain, indicating maximum inundation-affected areas, and was used for validating the results of the flood-plain landform classification. The 2001 image is covered largely by clouds, so it was used for validation instead of the 2008 image. The SRTM DEM was used to calculate average elevation and standard deviation of elevation via landform objects.

4.3.2 Removing the effect of land cover of the SRTM DEM in urban and vegetated areas

Before calculating local land-surface parameters, the SRTM DEM must be corrected for actual ground elevation. To define urban and vegetated areas, where bias in SRTM DEM exists, the land cover classification from the November 11, 2000, Landsat ETM+ was used to correct the SRTM DEM obtained in the same year. Land cover types were classified using an integrated method. Fractional images (high albedo, low albedo, vegetation, soil) obtained using a linear unmixing technique, the supervised classification image, MNDWI, and Land Surface Temperature (LST) were combined to produce a land cover image using a decision tree model. The spectral unmixing

technique including endmember selection and impervious surface estimation, has been described in many studies (Lu and Weng, 2006; Small, 2001; Wu and Murray, 2003). Integrating this technique with the conventional methods significantly reduced mixed-pixel problems, efficiently distinguished urban (impervious surface) from bare soil, and improved the land cover classification compared to application of a single method. Land cover classification was then verified with results from Pham and Yamaguchi (2007) and the land use classification dataset from 2000 generated by the Department of Remote Sensing technology, GIS and GPS, with an accuracy of 85%.

Preprocessing of the SRTM DEM was generally similar to the procedure used by Ho et al. (2012), including (1) eliminating the overestimated elevation in the entire low plain and (2) removing bias from trees and houses (Fig. 30). However, the second procedure was unlike that of the previous study, in which the SRTM DEM simply subtracted a constant height in the areas covered by trees and houses. The previous study area (central Vietnam) is a rural-dominated region and, as a result, the height of houses and trees was assumed to be constant. In the present study, the second step was carried out as follows:

i) In urban and forested areas, actual elevations of the SRTM DEM window were assumed to be the lowest elevation within a moving window (Funabashi et al., 2003).

$$z_i = \min_{i \epsilon C} z_i \qquad (7)$$

where z_i is the elevation of the SRTM DEM of pixel i within the 3 x 3 moving window C.

ii) In the central urban area, the SRTM DEM after step (i) was adjusted for

residual height caused by the artificial urban base.

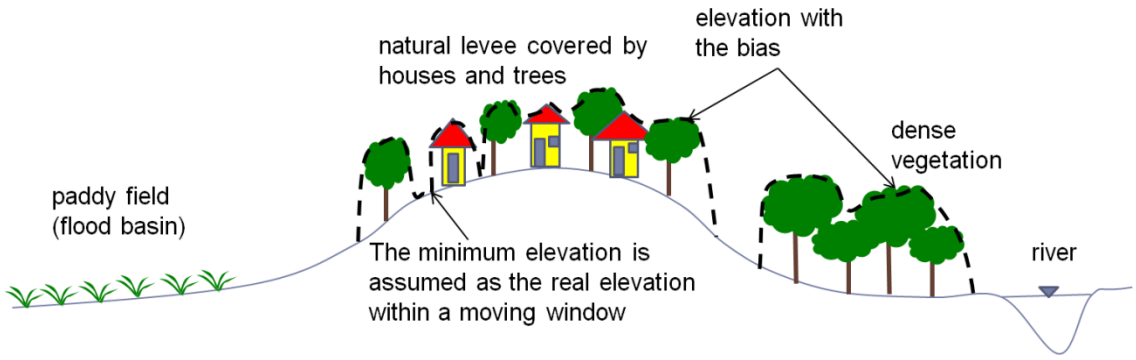

Fig. 29. Illustration showing the SRTM DEM bias resulting in an overestimation of elevation in urban and dense vegetation areas and explaining the preprocessing in step (i).

4.3.3 Floodplain landform classification using the rule-based method

In general, the rule-based landform classification relative to flood inundation mechanisms is based on Ho et al. (2012), conducted in the Vu Gia-Thu Bon alluvial plain in central Vietnam. The main purpose of the classification scheme is to identify moist areas (using MNDWI), which can be low compared to adjacent areas and easily absorb and maintain water and/or moisture (water and moist soil), and to classify the remainder of areas (non-water) into landform types that are little or not at all inundated. In short, this method includes three main procedures: (1) classifying moist conditions by dividing the MNDWI of a selective rainy-season image into separate water, moist soil, and non-water features independent of topographic features, surface gradient, and absolute elevation; (2) dividing objects into smaller units based on average elevation, land cover characteristics, and channel extraction using the r.param.scale function in GRASS GIS; and (3) designating final-level objects as landform categories using thresholds of average elevation, local edge reliefs, and relative position indices (Ho et al., 2012). However, in plains with low relief, such as Hanoi, elevation ranges at the

boundaries of landform objects are relatively low, and local relief in these cases is not useful for identifying elevated landforms (terraces, natural levees). Although terrain relief can be observed by visual interpretation, the threshold of local relief in Hanoi is not useful for the classification. To adapt to Hanoi, which is flat with very low relief, local relief was replaced by the average elevation and standard deviation of elevation calculated for each non-water object. Standard deviation (SD) of elevation is more stable than local relief (Evans, 1998). The purpose of using average elevation and SD of elevation is dividing non-water objects into homogeneous objects in terms of topographic variation. The final procedure was designating final-level objects into specific landform types using thresholds of average elevation (absolute and relative), the SD of elevation, land cover characteristics and relative position. Moist soil and inundated areas were extracted from the Landsat flood image of November 10, 2008. This flood image was captured a week after the heavy rain (Fig. 31).

$$SD = \sqrt{\frac{1}{n-1}\sum_{i=1}^{n}(z_i - \bar{z})^2} \qquad (8)$$

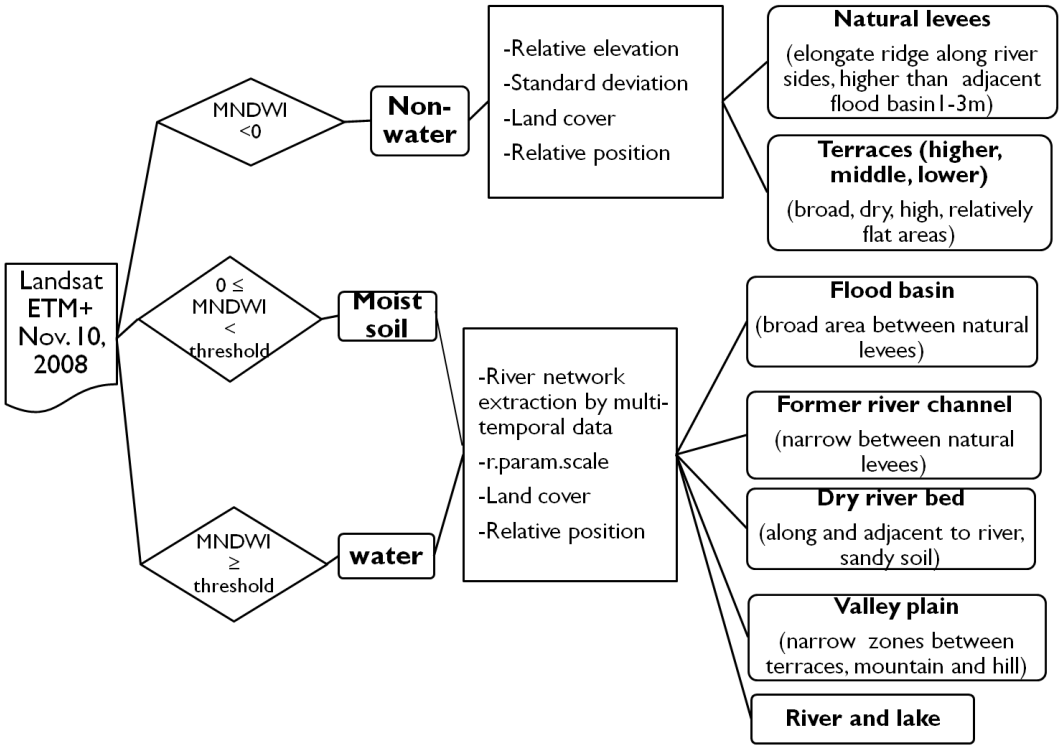

Fig. 30. The modified rule-based method in this study.

4.4 Results and discussions

4.4.1 Validation of the enhanced SRTM DEM and the landform classification result

The original SRTM DEM, before correction, shows bias that is coincident with the urban and tree cover patterns displayed in the land cover classification. After correction, the SRTM DEM bias is remarkably improved (Fig. 31).

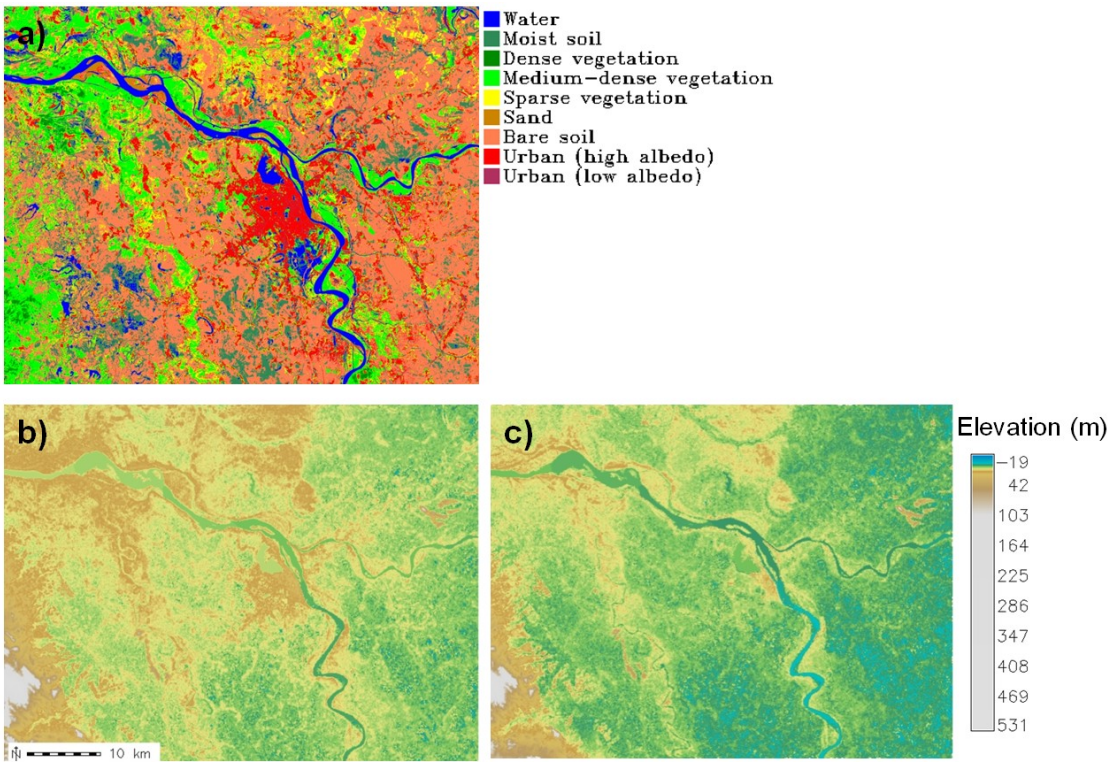

Fig. 31. Using the land cover classification image from 2000 (a) to correct the original SRTM DEM and remove bias caused by trees and houses (b) and the SRTM DEM after correction (c) with significant removal of the bias.

A statistical comparison between the SRTM before and after correction and the Hanoi DEM (15 m spatial resolution) from the Vietnamese Remote Sensing Center was conducted to verify the correction described previously. The comparison was performed within a 5 km radius from the urban center, where the DEM is available and the SRTM DEM bias is most significant. The bias of the entire area before correction is 2.4 m, whereas the biases of the four central districts (Hoan Kiem, Hai Ba Trung, Dong Da, and Ba Dinh) and outside of these four districts are 4.5 m and 2 m, respectively. These numbers can be explained by the significant effect of urban foundations and buildings in central districts, where population density and building height are much higher than other areas.

$$\text{BIAS} = \text{average}[\text{DEM}_{\text{SRTM}} - \text{DEM}_{\text{REF}}] \quad (9)$$

(Guth, 2006; Hofton et al., 2006).

Figure 32 shows profiles from the SRTM DEM before and after correction and the 15 m DEM crossing the Hanoi urban fringe and adjacent suburban areas. The upper diagram shows the bias caused by urban buildings in the urban fringe of Hanoi versus suburban areas.

SRTM DEM correction reduced the bias significantly in the entire area, with a mean error of -0.2 m, and the enhanced biases in the four central districts and adjacent suburban areas are 0.3 m and -0.1 m, respectively.

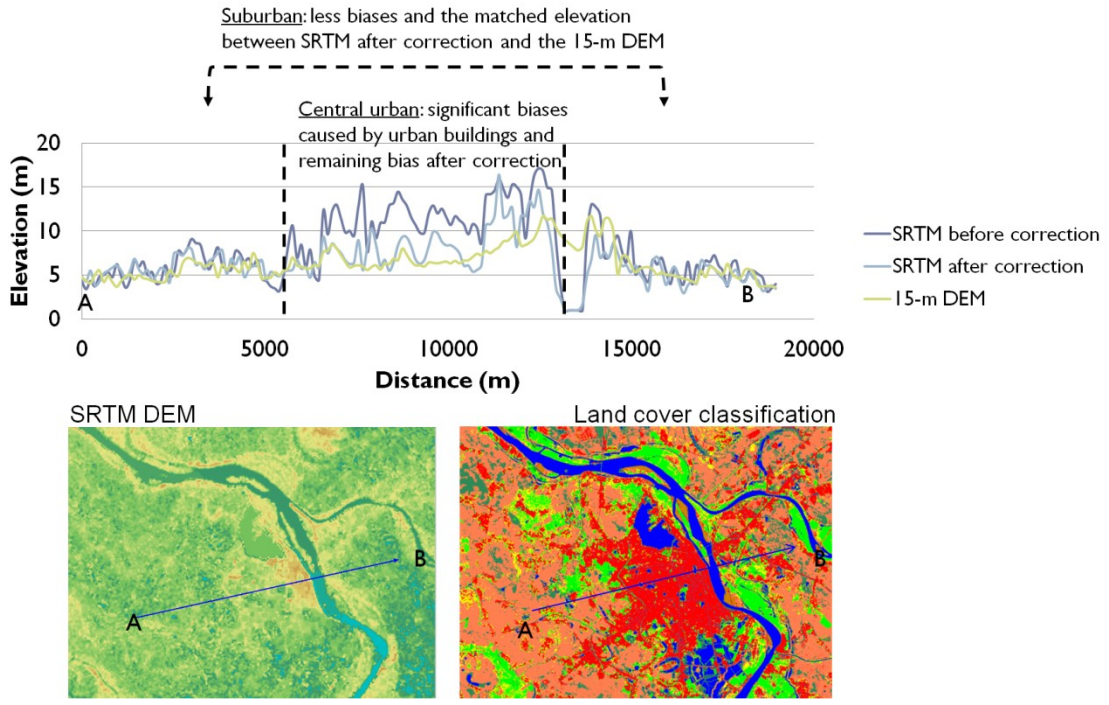

Fig. 32. Comparison of the SRTM elevation before and after correction, with the 15 m DEM of Hanoi crossing the urban fringe and suburban areas.

4.4.2 Visual comparison of the landform classification map by this method and the manual map by Funabiki et al. (2007)

The overall result of the modified, rule-based landform classification method is shown in Fig. 33a. This map was compared visually to the landform delineation result of Funabiki et al. (2007) using aerial photographs, satellite images, and geological maps combined with the SRTM DEM (Fig. 33b). This preliminary verification shows reasonable agreement between the present map and the manual map of Funabiki et al. (2007). In addition, landform properties in this floodplain obtained independently from the classification map and the SRTM DEM are similar to geographic descriptions of the Red River delta (Mathers et al., 1996; Mathers and Zalasiewicz, 1999; Tanabe et al., 2003; Funabiki et al., 2007 and 2012). The western alluvial floodplain of the Red River delta is characterized by the following:

- Alluvial terraces (Pleistocene) located in the northern and western areas.
- Large natural levees (maximum width 10 km near Hanoi) along meandering rivers, including the major tributaries of the Red River, Day River, and Duong River. The relative elevation of natural levees is 2–5 m higher than that of the adjacent back swamp (flood basin).
- Flood basin zones (back swamp) formed between natural levees or terraces and levees. The elevation of the flood basin between the Red River and Day River (northwest) is 3–5 m, but it is only 2–3 m in the eastern flood basin.

However, this method can classify more detailed levels of natural levees and the flood basin based on absolute and relative elevations; hence, the flood inundation states can be explained.

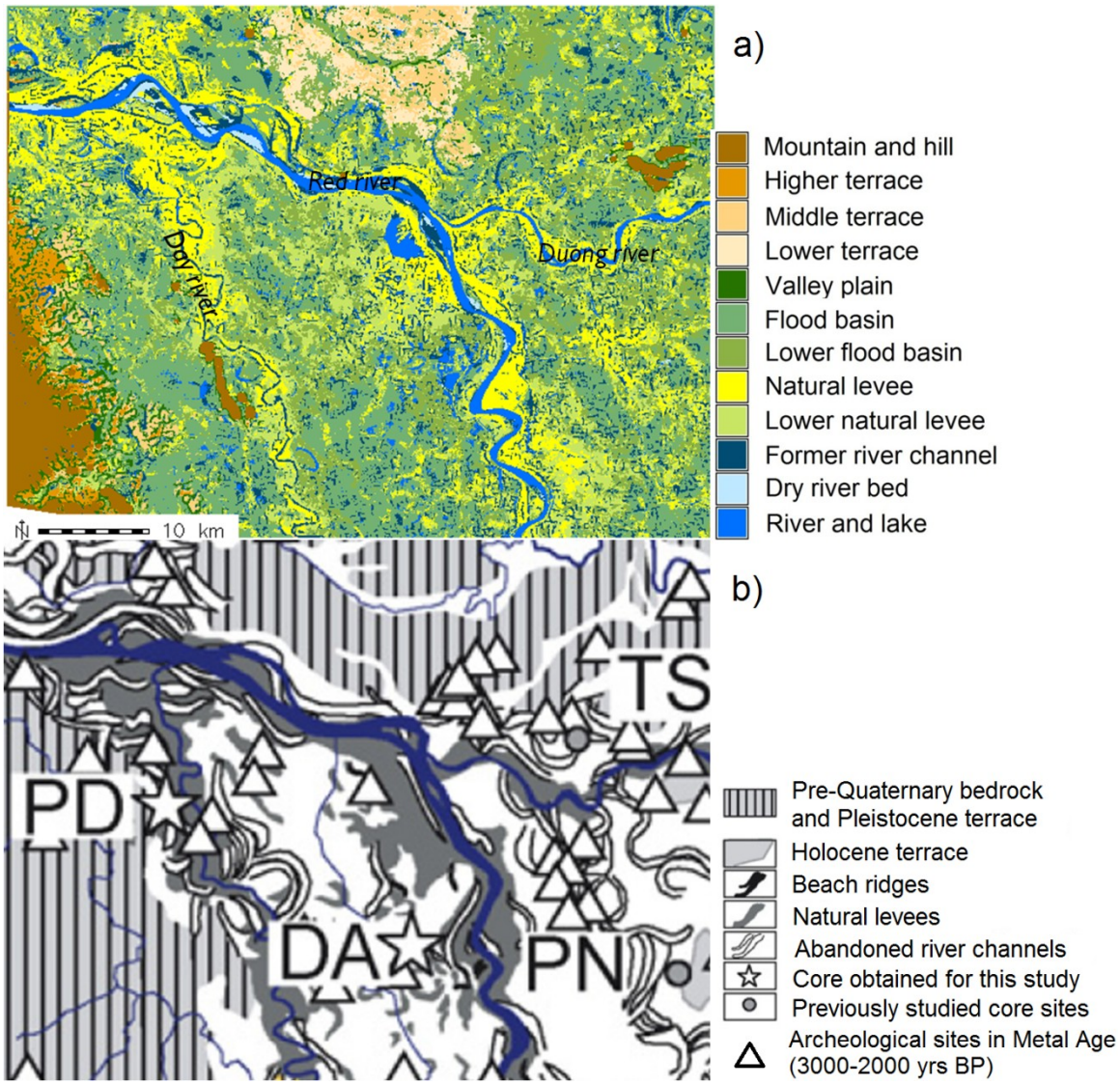

Fig. 33. Comparison of the landform classification map (a) generated by the modified rule-based method with the landform delineation result (b) of Funabiki et al. (2007).

4.4.3 Validating landform classification by flood inundated areas

The boundary delineation of landforms by the rule-based method is unbiased, which is an advantage of the method. It is also necessary to demonstrate the efficiency of this method in producing landform classifications versus manual results. To validate the landform classification results relative to flood-inundation conditions, a comparison

between landform units and inundated/non-inundated areas was conducted based on the relationship between landforms and flood inundation (Fig. 34). This comparison verified the boundary of the landform delineation by the flood-affected boundary. The July 18, 2001, Landsat ETM+ image, during a period of heavy rain causing a severe flood event in the Red River delta, was used to validate the landform classification results. This image may show the maximum possible flooded area. This image also was affected by cloud coverage in many areas of the urban fringe and the northern part, so it is not suitable for classification input, unlike the 2008 ETM+ image, but it is ideal for validation (Fig. 34B). A quantitative comparison between each landform and flooded areas was conducted within a cloud-free patch. Inundated and non-inundated areas in the 2001 ETM+ image were classified by dividing the MNDWI. Based on the characteristics of each landform corresponding to each flood-inundation state (Oya, 2001), the unsubmerged group, including higher and middle terraces, has inundated-area percentages of 0.6% and 10.4%, respectively, which is correlated to their flood-affected characteristics. The natural levee has 12.3% inundation, and the lower natural levee has a higher percentage of inundation (49.6%). In contrast, flood basins (91.6%), former river channels (76.1%), dry river beds (72.6%), and valley plains (70.4%) were dominated by inundation. The inundation percentage of the higher flood basin (58.1%) was lower than in the flood basin (Fig. 35).

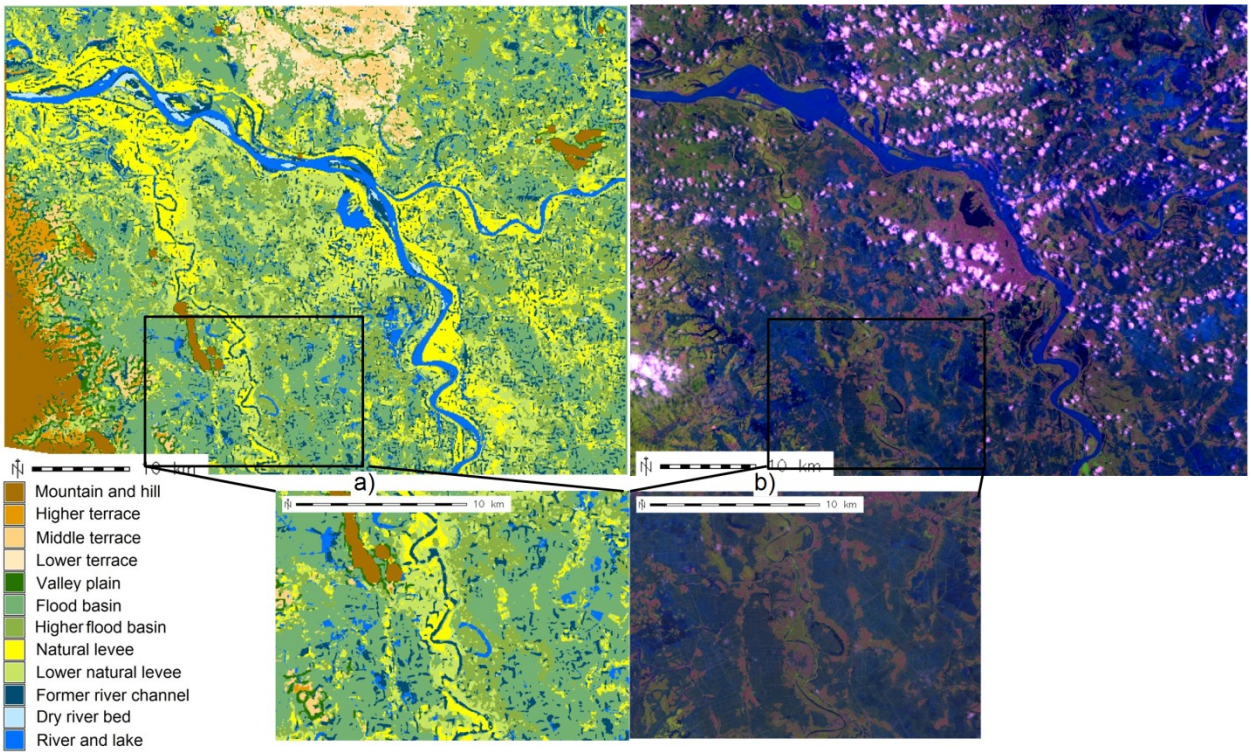

Fig. 34. Verification of the landform classification boundary (a) using the flood image from 2001 (b) in a cloud-free patch revealing similarity between landform units and flood inundation.

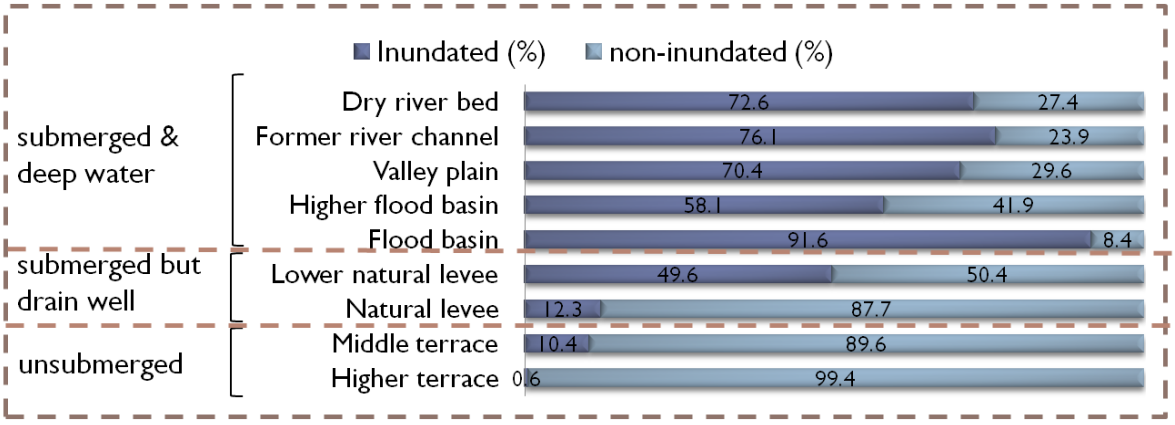

Fig. 35. Percentages of flood inundation for each landform unit correlated to flood conditions. This quantitative comparison was conducted for the small area in Fig. 34.

This comparison demonstrates the efficiency of the rule-based versus manual results; the rule-based method illustrates the current landform states comprising natural morphologic features and artificial effects, despite the SRTM DEM enhancement. Dehn et al. (2001) suggested that landforms are a result of either past geomorphic and geologic processes or a controlling boundary condition for actual geomorphic processes. In fact, the current flood inundation does not strictly follow the original landforms but is also constrained by the present, artificial landform boundaries.

4.5 Conclusions

The rule-based, small-scale landform classification method in the Red River's alluvial floodplains is based on key factors, including moisture conditions, local land-surface parameters, and relative position indices. Moist conditions classed in this study represent landform groups in floodplains and are independent of topographic features, such as surface gradient and absolute elevation. Thus, the moisture classification procedure can be applied to most floodplains to classify small-scale landforms. In areas where landform boundaries have clear elevation differences, such as in central Vietnam, local relief is useful for identifying elevated landforms (terraces, natural levees). In areas with flat and very low relief characteristics, such as Hanoi, average elevation and standard deviation of elevations are more applicable. Rules and parameters used in specific cases are flexible but based on the main ideas for classification; i.e., understanding the natural characteristics of a floodplain. Results of land cover classification support significantly to improve the SRTM DEM as much as removal of the elevation bias. Actual digital-terrain SRTM is very important for small-scale landform classification. Based on the relationship between small-scale landforms and flood conditions in alluvial floodplains, past

flood images can be used to validate rule-based landform classification results. In particular, boundary delineation of landforms using the rule-based method was verified as an advantage of this method compared to conventional, manual methods.

CHAPTER 5 – General conclusions

Flood hazard mapping has been increasingly concerned for the last recent decades, particularly due to the recent climate change. Flood inundation has been assessed by various methods. Although advanced techniques for modeling stages and levels of flood inundation have been developed, those techniques and methods require detailed hydro-meteorological data sets and/or high-resolution remotely sensed data. However, in developing countries, such detailed hydro-meteorological, topographic, and high-resolution data are often insufficient, inconsistent, and/or difficult to obtain. Therefore, using alternative data sets and suitable methods is very important. This study demonstrates that flood hazard mapping by using medium-resolution satellite images such as Landsat, ASTER data, and SRTM DEMs is an efficient and economical method and can be applied advantageously in alluvial floodplains. These data are available without or less cost and rather easy to access and analyze.

To achieve the goal of flood inundation assessment utilizing medium-resolution and available data, this study designates a geomorphological approach for flood susceptibility assessment. This study proves the effectiveness of flood hazard assessment based on the geomorphological approach using the SRTM DEM and medium-resolution multi-spectral data (Landsat and ASTER). Spectral images provide valuable information of soil moisture distribution indicating degrees of water absorbing capacity that reflects various types of small-scale landforms related to flood inundation conditions. The SRTM DEM provides information of elevations (absolute and relative) and terrain relief (local relief and standard deviation of elevation). The results of landform classification in the Thu Bon alluvial plain using this method corresponded with field investigation. The descriptions of geomorphological characteristics of

the alluvial in central Vietnam derived from the landform classification were consistent with those observed in field survey. In addition, flood height measured by field investigation was consistent with the prediction acquired from the landform classification. The field survey confirmed the correspondence and good fit between the observed landform characteristics and flood conditions. Moreover, the results revealed a close relationship between the geomorphological characteristics and flood conditions of the region. Flooding and sedimentation mechanisms create dynamic fluvial and coastal landforms, and these geomorphological features, in turn, affect the flood hazard potential. In particular, the utilization of the open-source GRASS GIS effectively supports to maximize, highlight, and visualize terrain relief, landforms in a sophisticated manner.

Due to significance of the detailed classification of landforms for predicting flood inundation as well as other natural disasters, generating more consistent and objective landform classification is considered. This study affirms that digital landform classification extracting landform objects processing remotely sensed multi-spectral/temporal and DEMs is more objective, time-saving, and convenient to edit versus the manual method by visual interpretation. The rule-based digital method for landform classification in the same study area (central Vietnam) demonstrated those advantages and provided highly consistent results with that created manually. The rule is based on modeling the inputs derived from the SRTM DEM and multi-temporal satellite images (moisture classification using MNDWI, land cover characteristics, local relief, average elevation, channel features, and relative position indices) for classifying small-scale landforms in alluvial plains. This method effectively separated large-size objects with high accuracy as well as in some cases more precise than those by the manual method. There is just a limitation on classifying small-size objects due to spatial resolution limitation. However, such

small-object classification affects very little on the prediction of areas that are susceptible to flooding. Thus, the rule-based digital method is promising and suitable for assessing flood inundation and is able to produce landform classification maps consistent with the manual ones. However, it is crucial and more convincing to generalize the rule-based digital method for wider applications in other alluvial plains. Hence, this study successfully adapted this method to Hanoi and surrounding areas – the western Red River delta, north Vietnam. In short, the key factors of the rule-based small-scale landform classification method in alluvial floodplains are moist condition, local land-surface parameters, and relative position indices. The fact that moist condition classification and relative position analysis work well in Hanoi area, the author is confident that these two factors can be applied to most alluvial floodplains for the small-scale landform classification as long as researchers can obtain good images indicating remaining inundation traces. In particular, classification of moist conditions can effectively separate groups of landforms in floodplains independent of topographic features. Whereas, local relief, which is useful to characterize small-scale landforms in the central Vietnam, is not applicable in the north Vietnam due to flat terrain characteristics (relief of the central Vietnam is higher). This study demonstrated that standard deviation of elevations was an alternative parameter and more stable to extract elevated areas such as terraces and natural levees in most alluvial plains. Thresholds of each parameter in specific cases vary based on topographic characteristics of floodplains. This study asserted that the precise boundary delineation of landforms by the rule-based digital method was an outstanding advantage compared to the manual method that was verified well by the past flood image.

Last but not least, the correction of the SRTM DEM before calculating local land-surface parameters is indispensable. Land cover classification provides necessary information of areas

covered by trees and houses to remove the biases in those areas. Bare-earth digital-terrain SRTM is very important for the small-scale landform classification. However, the processes are also flexible due to the characteristics of each area (rural, urban).

REFERENCES

Allen, I.R.L. (1965). A review of the origin and characteristics of recent alluvial sediments. *Sedimentology*, 5, 89-191.

Badura, J. and Przybylski, B. (2005). Application of digital elevation models to geological and geomorphological studies - some examples. *Przeglad Geologiczny*, 53 (10/2), 977-983.

Baker V.R., Kochel R.C., and Patton P.C. (1988). *Flood geomorphology*. Wiley Interscience, Toronto (Canada), 503 p.

Ballais, J. L., Garry, G., and Masson, M. (2005). Contribution of hydrogeomorphological method to flood hazard assessment: the case of French Mediterranean region. CR Geosciences, 337 (13), 1120–1130.

Bernert, J.A., Eilers, J.M., Sullivan, T.J., Freemark, K.E., and Ribic, C. (1997). A quantitative method for delineating regions: an example for the western Corn Belt plains ecoregion of the USA. *Environmental Management,* 21, 405–420.

Berthier, E., Arnaud, Y., Vincent C., and Rémy F. (2006). Biases of SRTM in high-mountain areas: Implications for the monitoring of glacier volume changes. *Geophysical Research Letters,* 33, L08502, doi:10.1029/2006GL025862.

Biradar, C.M., Thenkabail, P.S., Gangodagamage, C., and Islam, A. (2003). *LANDSAT Enhanced Thematic Mapper (ETM+) Mosaic*. International Water Management Institute (IWMI), available online at: www.iwmidsp.org/dsp/rs-gis-data/River-basins/Limpopo/01-Landsat-ETM-30m-7band-basin-mosaic-file/ (accessed on May 29, 2008).

Blankson, E.J. and Green, B.H. (1991). Use of landscape classification as an essential prerequisite to landscape evaluation. *Landscape Urban Planning*, 21, 149–162.

Blumberg, D.G. (2006). Analysis of large Aeolian (wind-blown) bedforms using the SRTM digital elevation data. *Remote Sensing of Environment,* 100, 179-189.

Centre for Hydro-meteorology Quang Nam (2001). *Hydrological Characteristics for Quang Nam Province*. Chapter 6 Sediment Transport.

Central Committee for Flood and Storm Control (CCFSC) (2006). *National Strategy and Action Plan for Disaster Prevention, Control, and Mitigation in Vietnam: 2001 to 2020*. September. CCFSC, Hanoi. Vietnam.

Coops, N.C., Gallant, J.C., Loughhead, A.N., MacKey, B.J., Ryan, P.J., Mullen, I.C., and Austin, M.P. (1998). Developing and testing procedures to predict topographic position from Digital Elevation Models (DEMs) for species mapping (Phase 1). *Environment Australia, CSIRO Forestry and Forest Products*, Client Report, 271, 56 p.

Dang, N.M., Babel, M.S., and Luong, H.T. (2011). Evaluation of food risk parameters in the Day River Flood Diversion Area, Red River Delta, Vietnam. *Natural Hazards,* 56, 169–194.

Dehn, M., Ga¨rtner, H., and Dikau, R. (2001). Principles of semantic modeling of landform structures. *Computers and Geosciences*, 27, 1005–1010.

Demirkesen, A.C., Evrendilek, F., Berberoglu, S., and Kilic, S. (2006). Coastal flood risk analysis using Landsat-7 ETM+ imagery and SRTM DEM: A case study of Izmir, Turkey. *Environmental Monitoring and Assessment,* 131, 293-300.

Demirkesen. A.C. (2008). Digital terrain analysis using Landsat-7 ETM+ imagery and SRTM DEM: a case study of Nevsehir province (Cappadocia), Turkey. *International Journal of Remote Sensing,* 29 (14), 4173-4188.

Drăgut, L. and Blaschke, T. (2006). Automated classification of landform elements using object-based image analysis. *Geomorphology*, 81, 330-344.

Drăguţ, L. and Eisanka, C. (2012). Automated object-based classification of topography from SRTM data. *Geomorphology*, 141–142, 21–33.

Evans, I.S. (1998). What do terrain statistics really mean?. In: Lane, S.N., Richards, K.S., Chandler, J.H. (Eds.), *Landform Monitoring, Modelling and Analysis*. Wiley, Chichester, 119-138.

Funabashi, M., Setojima, M., Okazaki, R., Imai, Y., and Yamamoto, K. (2003). Investigation of tree height estimation in urban areas by using ASTER data. Proceedings of 35th Scientific Conference of the Remote Sensing Society of Japan, 199-200 (in Japanese).

Funabiki, A., Haruyama, S. Nguyen, V. Q., Pham, V. H., and Dinh, H. T. (2007). Holocene delta plain development in the Song Hong (Red River) delta, Vietnam. *Journal of Asian Earth Sciences*, 30, 518–529.

Funabiki, A., Saito, Y., Vu, V. P., Nguyen, H., and Haruyama, S. (2012). Natural levees and human settlement in the Song Hong (Red River) delta, northern Vietnam. *The Holocene,* 22 (6), 637 –648.

Gallant, A. L., Brown, D. D., and Hoffer, R. M. (2005). Automated mapping of Hammond's landforms. *IEEE Geoscience and Remote Sensing Letters*, 2 (4), 384-388.

Guth, P.L. (2006). Geomorphometry from SRTM: comparisons to NED. *Photogrammertric Engineering and Remote Sensing,* 72 (3), 269-277.

Hammond, E.H. (1954). Small scale continental landform maps. *Annals of the Association of American Geographers*, 44, 32–42.

Haruyama, S., and Shida, K. (2008). Geomorphologic land classification map of the Mekong Delta utilizing JERS-1 SAR images. *Hydrological Processes*, 22, 1373–1381.

Hengl, T. (2006). Finding the right pixel size. *Computers & Geosciences*, 32 (9), 1283–1298.

Ho, D. D. and Shibayama, M. (2009). Studies on Hanoi Urban Transition in the Late 20th Century Based on GIS/RS. *Southeast Asian Studies,* 46 (4), 532-546.

Ho, T. K. L ., Umitsu, M., and Yamaguchi, Y. (2010) Flood hazard mapping by satellite images and SRTM DEM in the Vu Gia – Thu Bon alluvial plain, central Vietnam. *International Archives of the Photogrammetry, Remote Sensing and Spatial Information Science*, 38 (Part 8), 275-280.

Ho, T. K. L . and Umitsu, M. (2011). Micro-landform classification and flood hazard assessment of the Thu Bon alluvial plain, central Vietnam via an integrated method utilizing remotely sensed data. *Applied Geography*, 31, 1082-1093.

Ho, T. K. L., Yamaguchi, Y., and Umitsu, M. (2012). Rule-based landform classification by combining multi-spectral/temporal satellite data, and the SRTM DEM. *International Journal of Geoinformatics,* 8 (4), 27-38.

Hofierka, J., Mitášová, H., and Neteler, M. (2008). Geomorphometry in GRASS GIS. In: Hengl, T. and Reuter, H.I. (Eds), *Geomorphometry: Concepts, Software, Applications.* Developments in Soil Science, Elsevier, 33, 1-28.

Hofton, M., Dubayah, R., Blair, J.B., and Rabine, D. (2006). Validation of SRTM elevations over vegetated and non-vegetated terrain using medium-footprint LiDAR. *Photogrammetric Engineering and Remote Sensing*, 72 (3), 279–286.

Hori, K., Tanabe, S., Saito, Y., Haruyama, S., Nguyen, V., and Kitamura, A. (2004). Delta initiation and Holocene sea-level change: example from the Song Hong (Red River) delta, Vietnam. *Sedimentary Geology*, 164, 237 –249.

Imamura, F. and Dang, V.T., 1997. Flood and typhoon disasters in Viet Nam in the half century since 1950. *Natural Hazards*, 15, 71–87.

Iwahashi, J. and Pike R. J. (2007). Automated classifications of topography from DEMs by an unsupervised nested-means algorithm and a three-part geometric signature. *Geomorphology*, 86, 409 – 440.

Jain, S.K., Singh, R. D., Jain, M. K., and Lohani, A. K. (2005). Delineation of flood-prone areas using remote rensing techniques. *Journal of Water Resources Management*, 19 (4), 333–347.

Kenny, R. (1990). Hydrogeomorphic flood hazard evaluation for semi-arid environments. *Quarterly Journal of Engineering Geology*, 23(4), 333–336.

Kingma, N.C. (2002). *Flood hazard assessment and zonation.* Lecture Note, ITC, Enschede, The Netherlands.

Klingseisen, B., Metternichtc, G., and Paulus, G. (2008). Geomorphometric landscape analysis using a Rule-based GIS-approach. *Environmental Modelling & Software*, 23 (1), 109-121.

Koch A. and Lohmann P., (2000). Quality Assessment and Validation of Digital Surface Models Derived from the Shuttle Radar Topography Mission (SRTM). *International Archives of Photogrammetry and Remote Sensing (IAPRS),* 33, Amsterdam, 2000. Accessed on September 20, 2008 at www.ipi.uni-hannover.de/uploads/tx_tkpublikationen/Paper620.pdf.

Kono, Y. and Doan, D.T. (1995). Effect of water control on rice cultivation in the Red River Delta, Vietnam: A case study in the Nhue River irrigation system. *Southeast Asian Studies*, 32 (4), 425-445.

Kubo, S. (2002). Geomorphological features of the Thu Bon River Plain, Central Vietnam, and their relations on Flood hazards in 1999. Ac*ademic research, School of Education, Waseda University*, 50, 1-12.

Kuuskivi, T., Lock, J., Li, X., Dowding, S., and Mercer, B. (2005). *Void Fill of SRTM Elevation Data: Performance Evaluations*, available online at: www.intermap.com/images/papers/void_fill.pdf (accessed on Jan 7, 2006).

Lastra, J., Fernández, E., Díez-Herrero, A., and Marquínez, J. (2008). Flood hazard delineation combining geomorphological and hydrological methods: an example in the Northern Iberian Peninsula. *Natural Hazards*, 45, 277–293.

Li, Z. (1988). On the measure of digital terrain model accuracy. *Photogrammetric Record,* 12, 873–877.

Lu, D. and Weng, Q. (2006). Use of impervious surface in urban land use classification. *Remote Sensing of Environment*, 102 (1–2), 146–160.

MacMillan, R.A., Pettapiece, W.W., Nolan, S.C., and Goddard, T.W. (2000). A generic procedure for automatically segmenting landforms into landform elements using DEMs, heuristic rules and fuzzy logic. *Fuzzy Sets and Systems*, 113, 81-109.

Mathers, S.J. and Zalasiewicz, J.A. (1999). Holocene sedimentary architecture of the Red River delta, Vietnam. *Journal of Coastal Research*, 15, 314 –325.

Mathers, S.J., Davies, J., McDonald, A., Zalasiewicz, J.A., and Marsh, S. (1996). The Red River delta of Vietnam. *British Geological Survey Technical Report* WC/96/02, 41 p.

McFeeters, S. K. (1996). The use of the Normalized Difference Water Index (NDWI) in the delineation of open water features. *International Journal of Remote Sensing*, 17 (7), 1425-1432.

Melton, F.A. (1936). An empirical classification of floodplain streams. *Geographical Review*, 26, 593-610.

National Institute of Meteorology, Hydrology and Environment (2007). *Brief on climate change on global and in Viet Nam*.

Neteler, M. and Mitasova, H. (2007). *Open source GIS: A GRASS GIS Approach*, Third Edition. The International Series in Engineering and Computer Science, 773, Springer, New York, 406 p.

Nguyen, H. (2007). *A study of flood hazard assessment in the Thu Bon Plain based on geomorphological method and GIS*. Ha Noi University of Natural Sciences, Ha Noi National University, 'Unpublished Masters/PhD Thesis'.

Nguyen, M. D., Mukand, S. B., and Huynh, T. L. (2011). Evaluation of food risk parameters in the Day River Flood Diversion Area, Red River Delta, Vietnam. *Natural Hazards*, 56, 169–194.

Oya, M. (1956).Topographical Survey map of the Kiso river basin showing classification of flood stricken areas. *Appended map of the Resources Council Reference data*, Prime Minister's Office (in Japanese).

Oya, M. (2002). Applied geomorphology for mitigation of natural hazards. *Natural Hazards,* 25 (1), 17-25.

Pham, M.H. and Yamaguchi, Y. (2007). Use of remote sensing to monitor urbanization of Hanoi City center. *International Journal of Geoinformatics*, 3, 55-61.

Quang Nam Committee for Flood and Storm Control (CFSC) (2009). *The Strategies for Integrated Natural Disaster Management in Quang Nam Province until 2020* (In Vietnamese), Tam Ky City, May 2009.

Reuter, H. I., Nelson, A., and Jarvis, A. (2007). An evaluation of void-filling interpolation methods for SRTM data. *International Journal of Geographical Information Science,* 21 (9), 983–1008.

Reuter, H.I., Hengl, T., Gessler, P., and Soille, P. (2008). Preparation of DEMs for Geomorphometric Analysis. In: Hengl, T. and Reuter, H.I (Eds), *Geomorphometry: Concepts, Software, Applications*. Developments in Soil Science, Elsevier, 33, 87 – 120.

Rodríguez, E., Morris, C.S., Belz, J.E., Chapin, E.C., Martin, J.M., Daffer, W., and Hensley, S. (2005). *An assessment of the SRTM topographic product.* Technical Report, Jet Propulsion Laboratory C-31639, NASA.

Rodríguez, E., Morris C.S., and Belz, J.E. (2006). A global assessment of the SRTM performance. *Photogrammetric Engineering and Remote Sensing,* 72 (3), 249–260.

Saadat, H., Bonnell, R., Sharifi, F., Mehuys, G., Namdar, M., and Ale-Ebrahim, S., 2008, Landform classification from a digital elevation model and satellite imagery. *Geomorphology*, 100, 453 – 464.

Shaikh, M.G., Nayak, S., Shah, P.N., and Jambusaria, B.B. (1989). Coastal landform mapping around the Gulf of Khambhat using LANDSAT TM data. *Journal of the Indian Society of Remote Sensing,* 17 (1), 41-48.

Shida K. and Haruyama, S. 2004. Flood evaluation in the Mekong River Delta using by Jers-1 SAR Data. *Japan Geographical Congress* Abstract 65, 78 (in Japanese).

Small, C. (2001). Estimation of urban vegetation abundance by spectral mixture analysis. *International Journal of Remote Sensing*, 22, 1305–1334.

Speight, J.G. (1974). A parametric approach to landform regions. *Progress in Geomorphology*, *Special Publication, Institute of British Geographers*, 7, 213–230.

Speight, J.G. (1990). Landform. In: McDonald, R.C., Isbell, R.F., Speight, J.G., Walker, J., & Hop, M.S. (Eds), *Australian Soil and Land Survey Field Handbook*, 3rd edition. CSIRO Publishing, 9–57.

Tanabe, S., Hori, K., Saito, Y., Haruyama, S., Vu, V. P., and Kitamura, A. (2003). Song Hong (Red River) delta evolution related to millennium-scale Holocene sea-level changes. *Quaternary Science Reviews*, 22, 2345–2361.

Tanabe, S., Saito, Y., Vu, Q.L., Hanebuth, T.J.J., Ngo, Q.L., and Kitamura, A. (2006). Holocene evolution of the Song Hong (Red River) delta system, northern Vietnam. *Sedimentary Geology*, 187, 29 –61.

Tran, P., Marincioni, F., Shaw, R., Sarti, M., and Le, V. A. (2008). Flood risk management in Central Viet Nam: challenges and potentials. *Natural Hazards*, 46, 119–138.

Umitsu, M., Hiramatsu, T., and Tanavud C. (2006). Research on the flood and micro landforms of the Hat Yai Plain, Southern Thailand with SRTM Data and GIS. *Transactions Japanese Geomorphological Union,* 27 (2), 205-219.

Van Westen, C. (1993). *GISSIZ: Training Package for Geographic Information Systems in Slope Instability Zonation*. Enschede, The Netherlands ITC Publication, 15, 245 p.

Verhagen, P. and Drăguţ, L. (2012). Object–based landform delineation and classification from DEMs for archaeological predictive mapping. *Journal of Archaeological Science*, 39 (3), 698–703.

Wang, Y., Colby, J.D., and Mulcahy, K.A. (2002). An efficient method for mapping flood extent in a coastal flood using Landsat TM and DEM data. *International Journal of Remote Sensing*, 23 (18), 3681–3696.

Wang, Y. (2004). Using Landsat 7 TM data acquired days after a flood extent on a coastal floodplain. *International Journal of Remote Sensing*, 25 (5), 959 – 974.

Willige, B.T. (2007). Flooding risk of Java, Indonesia. *Proceedings of Forum DKKV/CEDIM: Disaster Reduction in Climate Change,* October, 2007.

Wolman, M.G. (1971). Evaluating alternative techniques of floodplain mapping. *Water Resources Research,* 7, 1383–1392.

Wood, J. (1996). *The geomorphological characterisation of digital elevation models. Ph.D*. Thesis. (Leicester, UK: Department of Geography, University of Leicester), 185 p.

Wu, C. and Murray, A.T. (2003). Estimating impervious surface distribution by spectral mixture analysis. *Remote Sensing of Environment*, 84 (4), 493–505.

Zandbergen P. (2008), Applications of Shuttle Radar Topography Mission Elevation Data. *Geography Compass,* 2 (5), 1404–1431.

Zheng, N., Takara, K., Tachikawa, Y., and Kozan, O. (2008). Analysis of vulnerability to flood hazard based on land use and population distribution in the Huaihe River basin, China. *Annuals of Disaster Prevention Research Institute*, Kyoto University, 51 B (2008).

Xu, H. (2006). Modification of normalised difference water index (NDWI) to enhance open water features in remotely sensed imagery. *International Journal of Remote sensing*, 27 (14), 3025-3033.

Websites

http://grass.itc.it/ (GRASS GIS open software source, accessed on August 15, 2008)

http://glcf.umiacs.umd.edu/data/ or http://glovis.usgs.gov/ (LANDSAT sources, accessed on September 10, 2008 and April 2010)

http://www.reliefweb.int/rw/rwb.nsf/db900SID/JBRN-7WLDXF?OpenDocument (accessed on December 2, 2009)

http://srtm.csi.cgiar.org/SRTMdataProcessingMethodology.asp (SRTM source, accessed on September 10, 2008)

http://visualizationsoftware.com/3dem.html (3DEM software source, accessed on October 2, 2008)

https://big.geogrid.org/ (GEOGrid - ASTER source, assessed on April, 2010)

ACKNOWLEDGEMENTS

Firstly, I would like to express my utmost and deepest gratitude to my supervisor – Prof. Yasushi Yamaguchi for his great supervision and continuous encouragement during my Ph.D course at Nagoya University. I greatly appreciate his great support and open-minded instruction to let me be able to pursue my research interests and to help me think issues more critically. He always gave me prompt and careful corrections and good suggestions for my work although he is often busy. I gratefully thank to his immense kindness and patience to show me the right ways when I made mistakes. He gently comforted and kindly understood when I had troubles and confusions. Deeply thank to him, I could overcome step by step and fulfill my PhD research.

Secondly, I would like to show my sincere thanks and appreciation to Prof. Masatomo Umitsu – my Master course supervisor and the second instructor of my Ph.D research. Although he worked at Nara University, he kept supporting and instructing me on my Ph.D study. I really appreciate his great consideration on either academic and life matters.

I would like thank Prof. Takeuchi and Assoc. Prof. Hori for their valuable comments and suggestions to help me improve my Ph.D thesis.

My gratitude also expresses to Dr. Sasai and all friends in the Lab who gave me useful comments and suggestions in the Seminar of Remote Sensing group, who shared with me moments when we stayed and worked together at the Lab. In particular, my sincere thank sends to Pham Minh Hai-san, a very nice and helpful senior, for his great supports in my study and life since I came to Japan. I would like to thank Chen-san, a smart and kind-hearted friend, for his technical assistance and helpfulness in my study. I also thank to Kato-san, Uezato-san, Shi-san, and Zhang-san, who stimulated the Benkyoukai for learning and discussing Remote Sensing knowledge.

I would like to send my grateful thanks to Prof. Ha Quang Hai and Dr. Tran Tuan Tu – my undergraduate supervisors and other teachers at Faculty of Environmental Sciences, University of Sciences in Hochiminh City, Vietnam who always encouraged me to continue my research and supported me in research materials.

I deeply thank to Ministry of Education, Culture, Sports, Science, and Technology for providing the Monbukagakusho Scholarship from Master to Doctoral courses – an amazing chance to study abroad in Japan. Without the scholarship, I could not concentrate all time for my research.

I would like to thank Nagoya University Global COE program for bringing me a great chance to do multi-disciplinary research in environmental studies with various experts and students from various majors.

I wish to thank to all of the teachers and the staff of Graduate School of Environmental Studies for their help and guidance for my academic and administration matters.

I want to thank to my Vietnamese friends for sharing the happiness, joyfulness, difficulties, experiences, and all things in daily life, who have made my life more colorful and unforgettable.

Finally, heartfelt thanks and love go to my families, my parents, my parents in-laws, my sisters, my brothers who are my motivation to try harder, encourage me, and give me persistent loves, cares, and supports for everything in my life. In particular, my special and dearest thank goes to my husband for his great sacrifices to let me finish my study for such a long time from Master to Doctoral courses. He always gives me in-time assistances and continuously spiritual supports.

HO Loan Thi Kim

December, 2012